

# Forecasts of Possible Phytoplankton Responses to Elevated Riverine Nitrogen Delivery into the Southern Firth of Thames

Prepared by:  
Niall Broekhuizen, John Zeldis  
(National Institute of Water and Atmospheric Research Ltd.)

For:  
Environment Waikato  
PO Box 4010  
HAMILTON EAST

ISSN: 1172-4005

December 2005

Document #: 1060600



---

# Forecasts of possible phytoplankton responses to elevated riverine nitrogen delivery into the southern Firth of Thames

---

Niall Broekhuizen  
John Zeldis

*Prepared for*

Environment Waikato

NIWA Client Report: HAM2005-131  
November 2005

NIWA Project: EVW05291

National Institute of Water & Atmospheric Research Ltd  
Gate 10, Silverdale Road, Hamilton  
P O Box 11115, Hamilton, New Zealand  
Phone +64-7-856 7026, Fax +64-7-856 0151  
[www.niwa.co.nz](http://www.niwa.co.nz)

---

© All rights reserved. This publication may not be reproduced or copied in any form without the permission of the client. Such permission is to be given only in accordance with the terms of the client's contract with NIWA. This copyright extends to all forms of copying and any storage of material in any kind of information retrieval system.



# Contents

---

Executive Summary	ii
1. Introduction	1
2. Methods	4
2.1 Estimation of light attenuation in the Firth of Thames	4
2.2 Phytoplankton Modelling	5
2.2.1 Grid resolution	6
2.2.2 Hydrodynamic scenarios	6
2.2.3 Implementation of PAR attenuation	7
2.2.4 Boundary conditions, nutrient loading scenarios and initial conditions	10
2.3 Analysis of model results	11
3. Results	13
3.1 PAR Attenuation	13
3.2 Phytoplankton Modelling	18
3.2.1 Model recalibration	18
3.2.2 Simulation results: Effects of increased nutrient loading to the southern Firth	20
3.2.3 Robustness Analysis	28
4. Discussion	31
4.1 Plausibility of results: shallow water processes absent from the model	31
4.2 Caveats: other simplifying assumptions	34
4.3 Seasonality of response to loading	35
4.4 Robustness of conclusions	36
4.5 Further work	37
5. Acknowledgements	39
6. References	40
7. Appendix A. Point source nutrient loads (baseline scenario)	42
8. Appendix B. Summary illustrations of the results from the individual cruises from which light-attenuation was inferred.	46

---

Reviewed by:



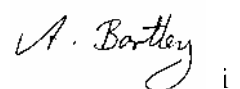
G. McBride

Approved for release by:



S. Elliott

Formatting checked



# Executive Summary

Landuse change in the catchment of the upper catchments of the four large rivers draining through the Hauraki plains is expected to lead to their being a greater delivery of nitrogen into the south-eastern Firth of Thames. Environment Waikato contracted NIWA to make forecasts of how increased nitrogen concentrations in the rivers feeding into the southern Firth of Thames might influence the likelihood that high standing stocks of phytoplankton would develop in the southern Firth of Thames.

After preliminary discussions, it was agreed that NIWA would undertake two pieces of work. Firstly, existing measurements of depth-specific light intensity (for the northern and central Firth of Thames) would be analysed with a view to developing an empirical predictor of the attenuation coefficient for Photosynthetically Active Radiation (PAR; for example, as a function of water-column depth and salinity). Secondly, NIWA's existing spatially explicit biophysical model (which simulates the dynamics of nutrients, organic detritus and three phytoplankton taxa) would be modified to incorporate the results of the attenuation analysis. The model would then be used to make a total of nine simulations (three nutrient-loading scenarios in each of three different months). The indicative budget for the project precluded any sensitivity analyses – though this report includes a very limited one. The simulation results were to be used to infer the consequences (for phytoplankton in the southern Firth) of increased nutrient loading. A nuisance-phytoplankton concentration threshold of 10 mg chl *a* m<sup>-3</sup> was defined as one standard against which to assess the influence of increased nutrient loading.

The three nutrient-loading scenarios were: 'baseline' (i.e., present situation), 'two-fold' and 'five-fold' – being respectively: two fold or five-fold increases in the concentrations of dissolved inorganic and total organic nitrogen passing down the Waihou, Waitoa, Piako and Ohinemuri rivers. Simulations were made under physical conditions (irradiance, riverflow, wind-conditions and hence current vectors, water temperatures and salinities) corresponding to September 1999, March 2000 and May 2003.

In simple regressions, the inferred light attenuation coefficient was found to be significantly correlated with water-depth (declining with increasing water-depth) and salinity (declining with increasing salinity). There was also a much weaker, positive relationship with chlorophyll concentration. There are significant cross-correlations between these explanatory variables, but in a multiple regression, both depth and salinity proved to be significant ( $P << 0.05$ ).

The resulting regression-model predictor of light attenuation was incorporated into the biophysical model. It proved necessary to perform an informal recalibration of the model such that it would produce plausible phytoplankton concentrations in the northern Firth (for which we have observational data).

The recalibrated model predicts high phytoplankton concentrations in the southern Firth (ranging from a space-time average of ~ 6 mg chl *a* m<sup>-3</sup> in May 2003 to in excess of 40 mg chl *a* m<sup>-3</sup> in March).

These concentrations are several times greater than are usually observed in the northern (cf southern) Firth of Thames. In the turbid, shallow, nutrient-rich, north-eastern Manukau harbour, chlorophyll concentrations are within the range 2-10 mg chl a m<sup>-3</sup> for most of the year, but sporadically rise to more than 60 mg chl a m<sup>-3</sup> during the summer months (Williamson et al. 2003). In the less enriched south-eastern Manukau, chlorophyll concentrations rarely exceed 10 mg chl a m<sup>-3</sup>. Given: (a) the relatively large area over which we are calculating average chlorophyll concentrations and, (b) the prolonged duration of the periods of high simulated chlorophyll, we suspect that, despite yielding plausible phytoplankton stocks in the northern Firth of Thames, our biophysical model is over-predicting 'basal' stocks (cf. short-lived 'blooms') in the very shallow, southern Firth. We describe several shallow-water-processes (absent in the present model) that would serve to reduce shallow-water standing stocks.

The model suggests that the system was not nitrogen limited in either September 1999 or May 2003. Thus, increased riverine nitrogen loads had little influence upon phytoplankton concentrations in those months. In contrast, for the March 2000 simulations, chlorophyll concentrations in the vicinity (to approximately 5 – 10 km) of the Waihou river-mouth are predicted to increase by 50 – 100% in the two-fold scenario and approximately 300% in the five-fold scenario. Diatoms and phytoflagellates increase much more dramatically than do dinoflagellates.

Whilst we are doubtful that phytoplankton abundances as high as those forecast would persist for long periods, we believe that the forecasts provide an indication of the 'worst-case' conditions that might arise sporadically. In the final section of this report, we identify several items of additional field- and simulation-work that would help to refine the forecasts that are presented within this report.



## 1. Introduction

Proposed land-use intensification in the upper catchments of the Waihou, Waitoa, Piako and Ohinemuri rivers makes it likely that nutrient inputs into the south-eastern part of the Firth of Thames will increase. Environment Waikato approached NIWA with a request that we make an assessment of the degree to which increased nutrient concentrations these rivers draining might modify phytoplankton concentrations in the southern Firth.

Following discussions between NIWA and representatives of Environment Waikato (Malene Felsing and Bill Vant), it was agreed that NIWA would: (i) analyse historical NIWA measurements of depth-specific light-intensity in order to derive estimates of the attenuation coefficient for photosynthetically active radiation. NIWA would then seek to establish a satisfactory empirical predictor for attenuation (e.g., as a function of local salinity and water-column depth). This relationship would be incorporated into NIWA's existing spatially resolved model of nutrient/phytoplankton dynamics in the Firth of Thames. The modified model would then be used to make 'forecasts' of phytoplankton concentrations in the Firth under three nutrient-loading scenarios for each of three nominal season/hydrodynamic conditions. The three nutrient loading scenarios were to be: (i) present situation ('scenario baseline'), (ii) a two-fold increase in nitrogen concentrations in the aforementioned rivers (scenario 'two-fold') and a five fold increase in concentrations (scenario 'five-fold'). In order to reduce the cost of the project, it was agreed that we would drive the nutrient/phytoplankton model with the output (half-hourly resolved time-series of current vectors, water-temperature and salinity) from pre-existing hydrodynamic simulations. The three seasonal/hydrodynamic regimes that were selected were: September 1999, March 2000 and May 2003. Within the indicative project budget, it was not possible to offer a sensitivity analyses, or an extensive recalibration of the model following the implementation of the new description of light attenuation.

The simulation results were to be used to infer the consequences, for phytoplankton standing stocks in the southern Firth, by comparison of e.g., time-averaged concentrations, coefficient of variation for concentration, number of days on which concentration exceeds the baseline average concentration, number of days on which the concentration exceeds  $10 \text{ mg chl } a \text{ m}^{-3}$ . The  $10 \text{ mg chl } a \text{ m}^{-3}$  threshold was nominated by Environment Waikato as a key value. Given the turbid nature of the southern Firth, chlorophyll-induced changes in water-colour are unlikely to become visible to the casual observer until chlorophyll concentrations approach this level (M. Gibbs, NIWA, *pers. comm.* 25 October, 2005).

We know of no nutrient or phytoplankton data for the very shallow (i.e., water less than approximately 5 m deep, Figure 1), southern Firth of Thames, but there are extensive field data from the northern Firth. These data indicate that phytoplankton production (and by inference, perhaps also standing stock) is frequently limited by low ambient concentrations of dissolved inorganic nitrogen (DIN). Whilst measured chlorophyll concentrations in the northern Firth of Thames have not exceeded 10 mg chl *a* m<sup>-3</sup>, Vant & Budd (1993) report several instances of chlorophyll concentrations in excess of 10 mg chl *a* m<sup>-3</sup> in the Manukau harbour. The Manukau is both shallow, and turbid, like the southern Firth but has substantially higher concentrations of DIN than have been recorded in the (northern) Firth.

Zeldis (2005) presented salt, carbon, nitrogen and phosphorus budgets for the Firth of Thames. He calculated that the Firth has an average flushing time of ~ 12 d, and that nitrogen entering the Firth through rivers and groundwater represented ~ 65% of the total nitrogen import. The remainder is supplied from the Hauraki Gulf. The latter supply is highly variable from year to year and Zeldis concluded that: “... *River and groundwater flows provided a ‘basal level’ of inorganic nutrient supply, whilst upwelling and downwelling offshore over the shelf generated most of the supply variation*”.

The largest rivers that drain into the Firth of Thames all enter around the Firth’s SE corner. With the exception of the Kaueranga, they also drain agricultural land. Thus, they carry high nutrient concentrations. Land-use intensification in their catchments is expected to raise these concentrations still further. Given that rivers (and groundwater) already dominate nitrogen delivery to the entire Firth of Thames, their influence can be expected to be still greater in the southern Firth. This, together with the observations that high algal concentrations have been reported in the similarly shallow and turbid, but more nutrient rich Manukau, raises the possibility that high algal concentrations (whether persistent or sporadic) may become a feature of the southern Firth of Thames should nutrient-inputs to the region increase.

The extensive data for the northern Firth of Thames were reviewed in Broekhuizen et al. (2002). They report that chlorophyll concentrations are moderately high by the standards of New Zealand’s coastal waters (median 1.9 mg chl *a* m<sup>-3</sup>), but do not cite any examples (or anecdotes) of algal blooms in the northern Firth. In the context of this report, the much shallower, southern Firth of Thames is the focus of interest. Unfortunately, we know of no data concerning either nutrient concentrations or chlorophyll concentrations for southern Firth waters shallower than five metre depth. Nonetheless, despite frequent boat movements in the immediate vicinity of Thames township, we are aware of no anecdotal reports of high algal concentrations.

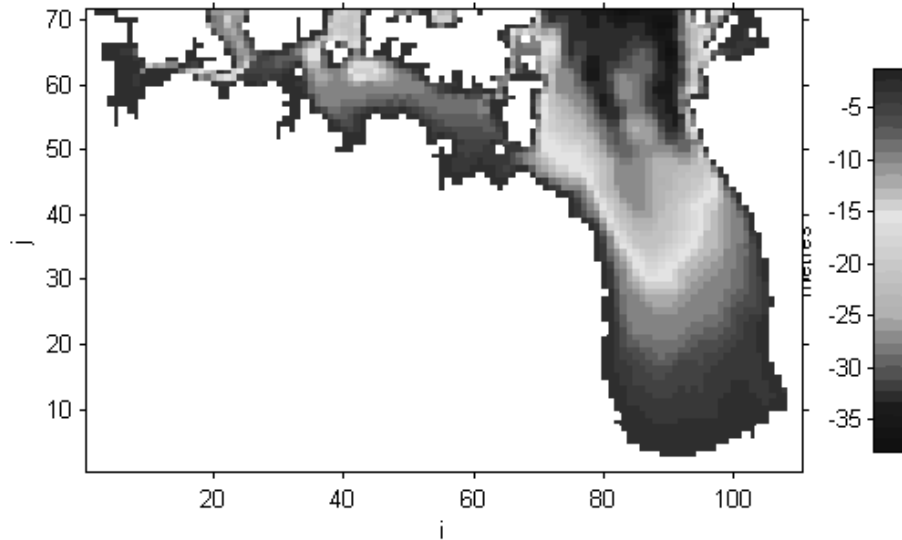


**Figure 1:** Bathymetry of the Firth of Thames and Tamaki Strait. This map is also a representation of the spatial extent of the domain used for the phytoplankton modelling. The tick-marks on the two axes indicate the distance (in model grid-cell units) from the domain's origin. Each model grid-cell is 750 m x 750 m horizontally. Thus, a J-coordinate of 10 equates to a displacement (in the y-direction) of 7.5 km from the origin.

## 2. Methods

### 2.1 Estimation of light attenuation in the Firth of Thames

Light attenuation through the water column from outer to inner Firth waters (> 5 m bottom depth) was sampled over a grid pattern of hydrographic sampling stations covering the inner/central to outer Firth (see Figure 3). Measurements were made during summer 2002, and autumn, winter, spring, and summer 2003, under NIWA FRST-funded Cross-shelf Exchange (C-SEX) research (Zeldis 2003; Zeldis et al. 2005). Depth-specific intensity of photosynthetically-active-radiation (PAR) was determined from Seabird Conductivity-Temperature-Depth (CTD) instrument profiles at each sampling site. Attenuation was determined using a log-linear fitting routine to the PAR-data from these CTD profiles. Each voyage had 10 to 17 profiles available for valid PAR attenuation determination. Quality control was based on goodness of fit of PAR data to the log-linear model (no estimates were used where the associated regression accounted for <94% of the variance in the data or where there were obvious ship shadow or other technical problems with the profiles (e.g., missing data, casts made in low light conditions i.e., less than approximately 1 hour after/before sunrise/sunset, respectively)). Other PAR quality control information is given in the Results section. Salinity was determined from CTD data and chlorophyll was determined from 250 ml GFF-filtered water samples collected at up to six depths (depending on bottom depth) on each profile, using spectrofluorometric determinations on acetone extracts.

We then sought relationships between the inferred attenuation coefficients and three probable explanatory variables that would be available within the biophysical simulation model. These were: salinity, bottom-depth, and chlorophyll concentration. The former two should be thought of as being likely proxies for light-attenuation due to turbidity enhanced scattering (increased photon path-length per vertical metre) and increased light absorption due to the presence of terrigenous dissolved organic material. The latter relates to light absorption by phytoplankton chlorophyll. Salinity and chlorophyll values for a station were calculated as the average of all samples taken between the sea-surface and the lesser of sea-floor-depth or 10 m (usually 2-3 samples).

Regression analyses were performed in the statistical package “R” (v. 1.5.1) using the glm algorithm for one-way regressions, and the nls algorithm for subsequent non-linear, multiple regressions.

## 2.2 Phytoplankton Modelling

We used a simulation model to simulate the dynamics of phytoplankton in the Firth of Thames. This model is described in Broekhuizen (Broekhuizen 1999; Broekhuizen & Oldman 2002; Broekhuizen et al. 2005), and has been shown to reproduce the temporal dynamics of phytoplankton in the north-eastern Firth of Thames (Broekhuizen et al. 2005). Minor bug-fixes introduced since those reports have not changed the model's behaviour greatly. The model simulates the dynamics of dissolved inorganic nitrogen (DIN, mg N m<sup>-3</sup>), dissolved reactive silicon (DRSi, mg Si m<sup>-3</sup>), the C, N & Si concentrations of suspended particulate organic detritus (mg C, N or Si m<sup>-3</sup>), the benthic density of these detrital materials (mg C, N or Si m<sup>-2</sup>) and the abundance of three phytoplankton taxa (diatoms, phytoflagellates and dinoflagellates). For each of the phytoplankton taxa, a track is kept of cellular abundance together with the C, N (and, for diatoms) cell-specific Si-content of these cells. Note also that in this application of the model, the so-called 'particulate organic detritus' also implicitly includes dissolved organic material.

Phytoplankton cellular growth is influenced by light intensity, water temperature and nutrient availability. Dinoflagellates are assumed to swim upwards when not nutrient stressed (when their internal nutrient quota is high), and downwards when stressed. Diatoms are neutrally buoyant when not stressed, and sink when stressed. Phytoflagellates are neutrally buoyant at all times. We adopted reflecting boundary conditions for phytoplankton at the sea-surface and the sea-floor. Unlike the two flagellate groups, diatoms require DRSi for growth (though this is dynamically irrelevant in the Firth, because DRSi is always plentiful). The phytoplankton physiological processes are parameterised from the literature. Diatoms have high maximum photosynthetic rates, and low respiratory rates. Phytoflagellates also have high maximum photosynthetic rates, but rather higher respiratory rates. Dinoflagellates have low maximum photosynthetic rates and high respiratory rates. Phytoplankton mortality rates are uncertain, and highly variable. Hall et al. (in review) estimated grazer-induced phytoplankton mortality to be 20–60% d<sup>-1</sup> (spring) and 40–90% d<sup>-1</sup> (summer) in the Hauraki Gulf. In earlier simulations with this model, values of 0.3 d<sup>-1</sup> for diatoms and phytoflagellates and 0.1 d<sup>-1</sup> for dinoflagellates have been found to yield plausible dynamics in the northern Firth of Thames and we have continued to use those values.

Upon death, modelled phytoplankton pass into the pool of suspended organic detritus. C and N within this pool remineralises at a rate of 5% d<sup>-1</sup>. Si remineralises at a very much lower, temperature dependent rate. The detritus also sinks at a fixed rate of 3 m d<sup>-1</sup>. Upon encountering the sea-floor, it enters the benthic detrital pool. This remineralises in the same manner as suspended detritus, but 14% (Giles 2001) of the

nitrogen remineralization flux is assumed to be lost to denitrification (rather than passing into the pelagic DIN pool).

The model is driven by: time-series of hydrodynamic conditions (temperature, salinity and current vectors), irradiance (Kirk 1983), together with 'oceanic' (i.e., at the interface with the Hauraki Gulf) and riverine boundary conditions for nutrients, detritus and phytoplankton (Appendix A). The hydrodynamic conditions were provided as the output of simulations made with the Danish Hydraulic Institute's MIKE3 model (Broekhuizen et al. 2005; Stephens & Broekhuizen 2003).

### **2.2.1 Grid resolution**

The biophysical model's horizontal spatial resolution is that of the hydrodynamic model - namely 750 m in the horizontal. In the vertical, the upper-most part of the water-column is represented with the same resolution as was used for the hydrodynamic modelling (namely: nominal 3 m surface layer followed by three layers of 2 m thickness). Where further layers are required before the sea-floor is reached, subsequent layers were integer multiples of the 2 m resolution used in the hydrodynamic model (namely 4 x 4 m, 2 x 8 m, 16 m). Note that: (i) whilst the surface layer of a water-column has a nominal thickness of 3 m, the instantaneous thickness will depart from this due to tidal variations and wind set-up. Similarly, the thickness of the bottom-most layer of each water-column is adjusted to match the bottom-bathymetry. In particular, the thickness of the bottom-most layer is constrained to lie in the range  $\Delta z_{\text{default}} \pm 0.5\Delta z_{\text{DHI}}$  (where  $\Delta z_{\text{default}}$  denotes the default thickness of the layer in question, and  $\Delta z_{\text{DHI}}$  denotes the thickness of a layer in the hydrodynamic model (2 m)).

### **2.2.2 Hydrodynamic scenarios**

Following discussions with Environment Waikato, it was agreed that simulations would be made for each of three different season/hydrodynamic situations, namely: September 1999, March 2000 and May 2003. These were chosen for two reasons. Firstly, hydrodynamic simulations for these periods already existed (Broekhuizen et al. 2005; Stephens & Broekhuizen 2003). Secondly, they span a range of environmental conditions: from spring (when waters are cold and unstratified, moderate insolation and inorganic nitrogen is plentiful), through summer (warm waters, stratified waters, plentiful insolation, low ambient concentrations of nitrogen in the northern Firth) through to late autumn (intermediate water temperatures, weaker stratification, low insolation and moderate inorganic nitrogen concentrations in the northern Firth).

In the case of the May 2000 scenario, the hydrodynamic simulations referred to in Appendix A of Broekhuizen et al. (2005) were used because the verification exercise

described in that report demonstrated that these provided a better fit to the data than did the hydrodynamic simulations made with the original parameterisation. The September 1999 and March 2000 simulations have not been rerun with the revised parameterisation. It is worth noting that whilst the performance of the hydrodynamic model on both the eastern (Broekhuizen et al. 2005) and western (Oldman et al. 2005) sides of the northern Firth has been verified, its performance in the southern Firth has not. In this respect, during the course of this project it became clear that, because interest had been focussed upon the deeper, northern Firth when the model was originally developed, its developers chose to eliminate inter-tidal zones by (artificially deepening the local bathymetry) in order to render the model numerically more tractable. Some possible implications of this simplifying assumption is discussed in section 4.1.

The March 2000 and May 2003 hydrodynamic simulations each spanned approximately 20 d. The September 1999 simulation spanned 25 d. When making the biophysical simulations for March 2000 and May 2003, we chose to recycle the final six-days' worth of hydrodynamic simulation in order to generate biological results spanning 25 days (giving the biological model longer to evolve responses to the differing riverine forcing).

### 2.2.3 Implementation of PAR attenuation

In reality, the attenuation of light in pure water is strongly wavelength dependent - light from the red end of the visible spectrum is absorbed more rapidly than light from the green end (pure water attenuation coefficients are approximately  $0.4 \text{ m}^{-1}$  and  $0.078 \text{ m}^{-1}$  respectively). At the sea-surface they each represent 50% of the total PAR, but one expects that the green component should become increasingly dominant with increasing distance from the sea-surface. Failure to account for the differential absorption results in erroneous predictions of depth-specific total PAR. For this reason, the model makes a distinction between 'red' and 'green' PAR constituents.

The empirical predictor of PAR attenuation (sections 2.1 and 3.1) predicts the attenuation coefficient for total PAR using water-column depth, depth-averaged salinity and near-surface chlorophyll as predictors. Whilst our method of inferring PAR-attenuation from the field data takes no explicit account of differential absorption, it is legitimate to think of it as a measure of 'green-light' absorption. In each vertical light-profile, the surface-most measurement of depth-specific PAR was made at 2 m point (from sea-surface) below the sea-surface. At this depth in pure water, 65% of the incident 'red' light would have been lost, but only 15% of the incident green light would have been lost. Thus, even at this depth, the total PAR is already green-dominated. For the biophysical model, we assumed that the empirically-

derived predictor of attenuation equates to the model's 'green-light' attenuation coefficient. We derived the model's red-light attenuation coefficient by adding a factor of 0.32 (pure-water red-light attenuation coefficient minus pure water green light attenuation coefficient) onto the intercept of the empirical model of light attenuation (but see the Sensitivity Analysis section for an alternative means of deriving the red-light coefficient).

There are three further departures between the manner in which light attenuation is calculated in the model, and in the empirical model. The first is as follows: the regression model predicts average attenuation over the entire water-column using (measured) near-surface (sea-surface to lesser of sea-floor or 10 m depth) average chlorophyll and salinity; in the model, attenuation is predicted on a layer-by-layer basis (2 m vertical resolution) using the layer-specific average simulated chlorophyll and salinity values. Simulated chlorophyll is derived from the simulated diatom, phytoflagellate and dinoflagellate concentrations assuming C:Chl ratios of 50:1 (by mass) for the former two groups and 100:1 for the latter. Modelled salinity is provided in the forcing data provided to the biological model as output from the hydrodynamic model. Measurements in the northern Firth of Thames indicate that near-surface and near-bed salinities usually differ by only approx. 0.1-0.2 psu, so our decision to use layer-specific salinity in place of the depth-averaged-salinity of the empirical relationship introduces only a small deviation. Similarly, measured chlorophyll concentrations in the deeper parts of the Firth (where near-surface and near-bed chlorophyll concentrations might be expected to differ) are such that chlorophyll induced attenuation would be negligible relative to background levels. Thus, our use of layer-specific chlorophyll also introduces only a small deviation.

The second difference between the manners in which the attenuation coefficient was calculated and the manner in which it was used stems from the fact that the simulation model extends into the very shallow (< 5 depth) southern Firth - for which we have no field measurements of the attenuation coefficient. In a water-column of zero depth, the empirical regression relationship (see Results) indicates that the attenuation coefficient will rise towards  $7 \text{ m}^{-1}$  as salinity drops towards zero – though it cannot climb above  $2.0 \text{ m}^{-1}$  provided that the salinity remains above 28 ppt. The maximum attenuation coefficient that we have measured in the Firth of Thames was  $2.05 \text{ m}^{-1}$  (measured at 5 m depth when stormy conditions were causing seabed material to 'boil to the surface'). For our simulations, we chose to assume that conditions leading to attenuation coefficients in excess of  $2.0 \text{ m}^{-1}$  would be infrequent and short-lived<sup>1</sup>. We therefore chose to 'cap' the predicted depth-and-salinity dependent component of the ('green') light attenuation coefficient at that value (additional, chlorophyll induced

---

<sup>1</sup> Vant (1991) reported the results of fortnightly monitoring over one year at four sites in the northern Manukau harbour. The annual mean estimates of the diffuse light attenuation coefficient varied between  $0.8 \text{ m}^{-1}$  and  $2.1 \text{ m}^{-1}$ . Maximum measured values were less than  $3 \text{ m}^{-1}$  – though subsequent modelling suggested that attenuation may exceed  $6 \text{ m}^{-1}$  on windy (=especially turbid) days.

attenuation may take the total (green) light attenuation above this threshold). The depth-and-salinity dependent component of the 'red' light coefficient was therefore implicitly clipped at a value of  $2.32 \text{ m}^{-1}$ . In practice this clipping is dynamically unimportant because salinities fall below 28 ppt only very close to the mouth of the Waihou (Figure 2).

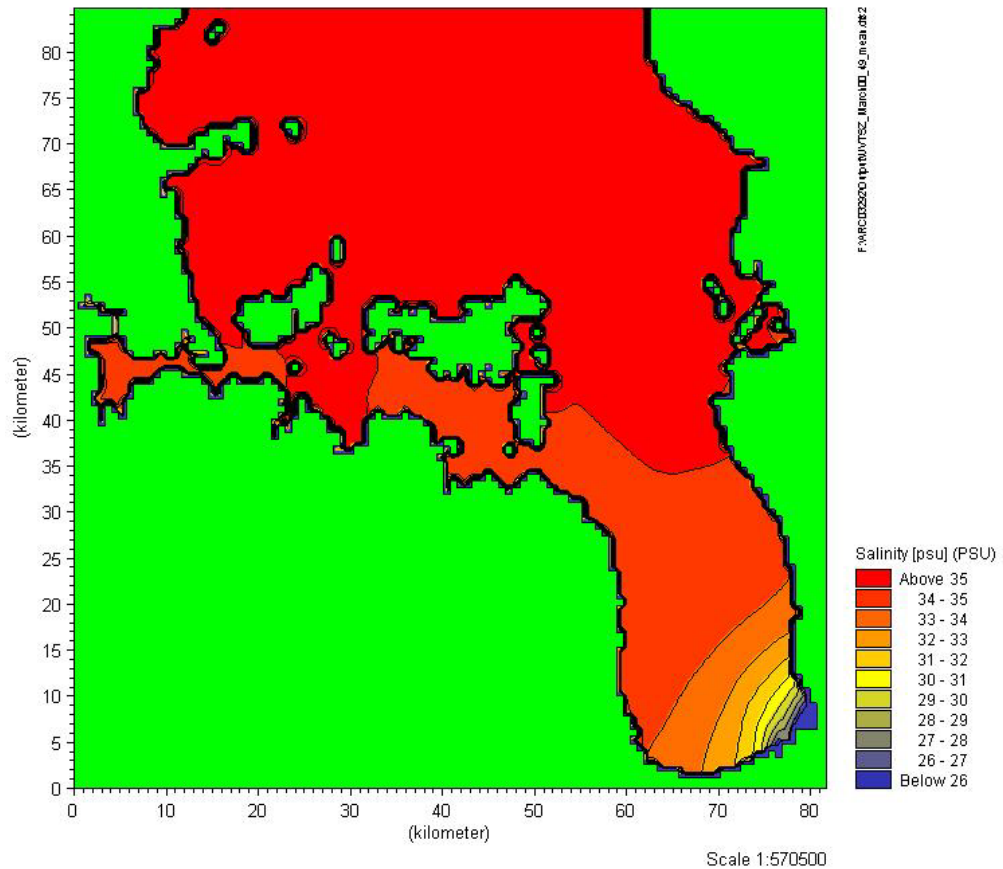


**Figure 2:** Time- and depth-averaged salinity in the Firth of Thames inferred from the March 2000 simulation.

The third departure between calculation and implementation of light attenuation was required upon learning that the initial conditions which had been used when making the May 2003 hydrodynamic simulations were horizontally homogenous. Even close to the river mouths the initial salinities were those more characteristic of the northern Firth (these hydrodynamic simulations were made in earlier projects in which interest had focussed upon the northern Firth). Thus, simulated salinities in the southern firth were initially too high. Since attenuation is negatively correlated with salinity in the default attenuation model (Eq. 2, page 15), this implies that the effective attenuation

coefficients in the southern Firth are too low. Inspection of the simulated salinities indicates that it took approximately six days for the 'plume' of low salinity water stemming from rivers to attain pseudo-steady state. To avoid excessive phytoplankton growth during this transient period, we instead adopted the empirical model of attenuation that was based upon depth and chlorophyll only (Eq. 3, page 15) for the first six days of the simulation.

#### **2.2.4 Boundary conditions, nutrient loading scenarios and initial conditions**

##### **Seaward boundary conditions**

Differing seaward boundary conditions are assumed for each of the three seasonal scenarios, but these are held constant for the duration of the simulation. In the case of the May 2003 simulation, the values were based upon field measurements. In the other two cases, they were chosen to be 'typical of the time of year'.

##### **Nutrient loading scenarios (point source boundary conditions)**

The model has point sources of inorganic and detrital nitrogen corresponding to the five main rivers flowing into the southern Firth. These are the Piako, Waihou, Waitoa, Ohinemuri and Kaueranga rivers. The Piako and Waitoa share a common river-mouth, as do the Wihou and Ohinemuri – however flow and nutrient data have been collected above the respective confluences. We have therefore chosen to represent them as distinct (but spatially coincident) sources in the model. The model also has a point source discharge corresponding to the sewage discharge from Thames township. All of the point sources were assumed to be devoid of phytoplankton.

All point sources were assumed to flow into the water-column's surface layer. Instantaneous nutrient loadings from each point source were derived from the product of an instantaneous flow and a concentration. Instantaneous flows and concentrations were derived from monthly-resolved data (Appendix A) provided by Environment Waikato by means of linear interpolation. For each of the three seasonal scenarios, we consider three nutrient loading scenarios: (i) 'baseline' (scenario 0); (ii) moderately elevated (scenario two-fold); (iii) greatly elevated (scenario five-fold). For the baseline scenario, the DIN and detrital N concentrations were those listed in Appendix A. In the other two scenarios the DIN and organic N concentrations in the Piako, Waitoa, Waihou and Ohinemuri rivers were elevated two-fold (scenario two-fold) or five-fold (scenario five-fold) relative to those of the baseline scenario. Following discussions with the client, it was agreed that we would assume that the point-source flow-rates remained the same in all three nutrient-loading scenarios (i.e., land-use change will not modify water-yield).

Point-source DIN entered the DIN pool of the appropriate control-volume within the model. Point-source organic N (particulate organic N + dissolved organic N) entered the suspended organic detritus pool of the receiving control-volume.

### **Initial conditions**

The initial conditions for nutrients, detrital material and phytoplankton were set equal to the corresponding boundary conditions – regardless of location within the Firth. Initial benthic detrital densities were set to 1.4 mg N cm<sup>-2</sup> of sea-bed. This figure is based upon preliminary analyses of recent NIWA benthic survey data from the northern and central Firth of Thames.

## **2.3 Analysis of model results**

We infer the possible consequences of increased nutrient-loading into the southern Firth by comparison of the simulated phytoplankton concentrations arising from the three nutrient-loading scenarios. This is done for each of the three seasonal scenarios in turn. For a given season, each of the loading scenario-simulations was started from the same initial conditions. We chose to exclude the first five days'-worth of simulation results in order to give the model some time to 'forget' its initial conditions and 'adjust' towards the state dictated by the riverine inputs (and other environmental conditions). It is however important to realise that because the model was driven by time-varying environmental conditions (insolation, temperature, and particularly current-vectors (day-to-day tidal residuals are very variable due to changing wind-fields), it is very difficult to determine how long the model's transient is. Zeldis (2005) has calculated that, for the entire Firth of Thames, the flushing time is approximately 12 d, but the smaller volume of the shallow, southern Firth, combined with the riverine inputs in this area suggest that it may flush more rapidly (though, countering these influences, tidal residuals tend to be smaller in the southern Firth). Inspection of simulation results (not shown) reveals that the standing stocks of nutrient and phytoplankton in the system usually change rapidly over the first three-to-five days, and evolve more slowly thereafter. Our decision to drop the first five days was pragmatic: retain sufficient data to permit robust statistics to be calculated, but drop sufficient to avoid the most rapid part of the initial transient.

We present the results from the simulation modelling in several ways. Firstly, we present maps of the time-and-depth-averaged concentrations of baseline-scenario DIN, and phytoplankton carbon in each taxon. Averaging was over the period days 6-25, and from the sea-surface to the lesser of sea-floor or 20 m depth. Accompanying these

maps we also present maps of change (relative to the corresponding baseline scenario) under the two-fold and five-fold scenarios. Relative change was calculated as:

$$R^j = 1 + \frac{1}{n} \sum_{i=6}^n \frac{E_i^j - B_i^j}{B_i^j}$$

In which  $E_i^j$  is the 24-hour average of the depth-averaged concentration of characteristic  $j$  (being DIN concentration or concentration of one of the three phytoplankton taxa) on day  $i$  of the elevated loading simulation.  $B_i^j$  is the corresponding concentration in the baseline scenario, and  $n$  denotes the total number of days in the simulation.  $R^j = 1.0$  indicates no change,  $R^j > 1.0$  indicates an increase relative to the baseline scenario, and  $R^j < 1.0$  indicates a decline relative to the baseline scenario. For the September and May seasons  $n$  was 25. For the March simulation, it was 23 days. For this month, the five-fold scenario proved to be much more numerically demanding than the other simulations. This simulation took several times longer to run than any of the others. After having been running for 28 CPU-days, a network failure caused the model to crash, and there was not sufficient time to rerun this simulation to completion. We do not believe that the results are materially altered by the loss of the final two days of simulated period.

In addition to the maps, we present a table listing the mean, median and coefficient of variation (CV) for simulated southern-Firth <sup>2</sup>chlorophyll concentration under each scenario. The table also lists the number of days on which the simulated one-day average chlorophyll concentration exceeded the 20 day (18 day for March 2003 simulation) average, and the number of days on which it exceeded 10 mg chl  $a$   $m^{-3}$ . In preparing this Table, EW and NIWA agreed (e-mail from Malene Felsing, Environment Waikato, 1 December 2004) that the analysis should be restricted to the southern Firth of Thames southern Firth of Thames (J-coordinate  $\leq 20$ , see Figure 1). As anticipated at that time, this did prove to be the region most impacted by the increased nutrient loadings.

---

<sup>2</sup> Chlorophyll concentration is not a state-variable of the biophysical model. We have calculated an approximate chlorophyll concentration using a weighted-sum of the simulated carbon concentrations of each of the three taxa. Even within individual species, C:Chl ratios vary (two – three fold) in response to the cell's physiological condition (as determined by ambient temperature, nutrient concentrations and PAR intensity). Dinoflagellates tend to exhibit higher C:Chl ratios than diatoms or phytoflagellates. We have adopted C:Chl ratios of 100:1 for dinoflagellates and 50:1 for the diatoms and dinoflagellates.

## 3. Results

### 3.1 PAR Attenuation

After exclusion of data which were considered to be unreliable (for example, because of ship shadow effects or unusually stormy conditions), there were 69 estimates of the attenuation coefficient for PAR available from the field data. They spanned a depth range of 5 m to 42 m, a salinity range of approx. 32.8 – 35.1 ppt, and chlorophyll concentration of 0.17 – 4.4 mg chl *a* m<sup>-3</sup>. Within these data, the estimated attenuation coefficients ranged from 0.14 – 1.1 m<sup>-1</sup>. There were six outliers (in the range 1.4 – 2.05 m<sup>-1</sup>) amongst the rejected attenuation coefficient estimates. These were rejected as being atypically high for the mid to inner Firth locality. They were gathered (during the September 2003 voyage) under very rough sea conditions in which the bottom sediments were seen to be ‘boiling to the surface’.

Results from the voyages which enabled the light-attenuation coefficient to be calculated are presented in Figure 3 (average of all voyages), and Appendix B (results for the individual voyages). The attenuation coefficient (denoted *K*<sub>par</sub>) is clearly larger in the southern Firth, but the <sup>3</sup>euphotic depth invariably extends to the sea-floor in the southern Firth whilst failing to reach it in the northern Firth. This implies that at the sea-floor, 24-hour averaged net phytoplankton production is net positive in the southern Firth, but net negative in the northern Firth. Despite this, the depth integrated production is inferred to be greater in the deeper parts of the Firth.

---

<sup>3</sup>Strictly, the euphotic depth is defined to be the depth at which 24-hour averaged photosynthesis exactly balances 24-hour averaged respiration. We have adopted the common, pragmatic definition – the depth at which the PAR intensity is 1% of the surface PAR.

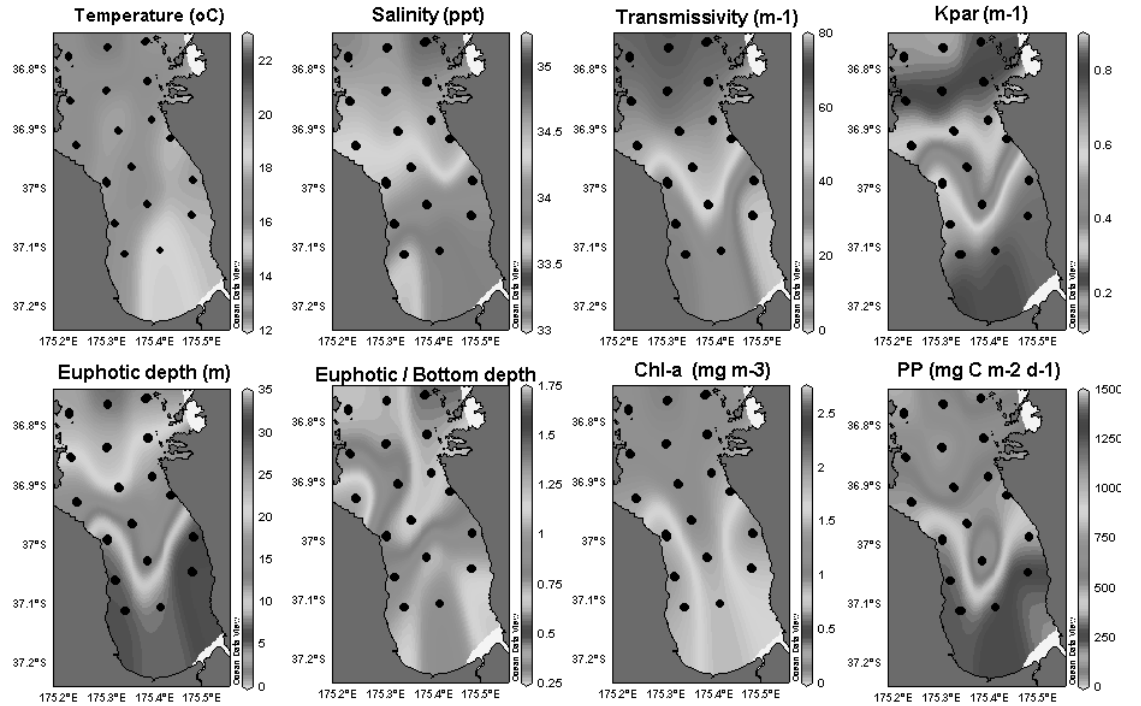


**Figure 3:** False-colour plots of water-column characteristics during the 5 seasonal voyages summer 2002-summer 2003. Black dots indicate the location of the sample stations.  $K_{par}$  denotes the inferred PAR-attenuation coefficient. PP denotes the estimated depth-integrated gross primary production. Temperature, salinity, transmissivity and chl-*a* are mean values over the upper 10 m (or less if bottom depth was < 10 m), and euphotic depth is the depth of 1% surface PAR. These plots were derived from the station-averages of the individual voyages; refer to Appendix B to see the results for each individual voyage.

Initial, simple regression analyses suggested that the attenuation coefficient declined with increasing depth ( $P < 0.001$ ) and increasing salinity ( $P < 0.001$ ), and increased with rising chlorophyll concentration ( $P < 0.01$ ). There were significant correlations between depth and salinity ( $P < 0.001$ ) and depth and chlorophyll ( $P < 0.001$ ) (Figure 4). Chlorophyll and salinity were not correlated.

A mixed linear (for salinity and chlorophyll) and exponential (for depth) multiple regression model was used to better-fit the data for the prediction of  $k_{PAR}$ . In this, the coefficient for the chlorophyll term proved to be non-significant. Thus, the most parsimonious, multiple regression model proved to be:

$$k_{PAR} = 7.25 - 0.221S + \exp(-0.014D) \quad \text{Eq. 1}$$

in which  $k_{PAR}$  is the attenuation coefficient ( $\text{m}^{-1}$ ),  $S$  is the depth-averaged salinity (ppt) and  $D$  is the water-depth (m). Using this model, the residual standard error is

0.147 and the deviance is 1.425 ( $r^2=0.75$ ). This model excludes chlorophyll *a* as a predictor. Nevertheless, for reasons which we clarify shortly, we have chosen to adopt an alternative model which retains chlorophyll (denoted *Chl*):

$$k_{PAR} = 7.328 - 0.226S + \exp(-0.0118D) + 0.0392Chl \quad \text{Eq. 2}$$

Whilst Eq. 2 does provide a slightly improved fit to the field data ( $r^2=0.76$  residual standard error=0.145, deviance=1.377), the improvement is negligible. Although the coefficient for the chlorophyll term is not statistically significant ( $P=0.13$ , cf  $P<0.001$  for the remaining coefficients), we have chosen to retain it to ensure that the remaining coefficients do not implicitly account for chlorophyll effects. This ensures that chlorophyll effects do not become ‘double-counted’ within the simulation model (which includes an attenuation term due to ‘self-shading’). The correspondence between predicted attenuation (using Eq. 2) and observed attenuation is illustrated in Figure 5.

As noted previously, for the first six days of the simulations we used a simpler regression-relationship that took no account of salinity:

$$k_{PAR} = 0.7669 \exp(-0.00416D) + 0.0307Chl \quad \text{Eq. 3}$$

(residual standard error=0.179, deviance=1.973).

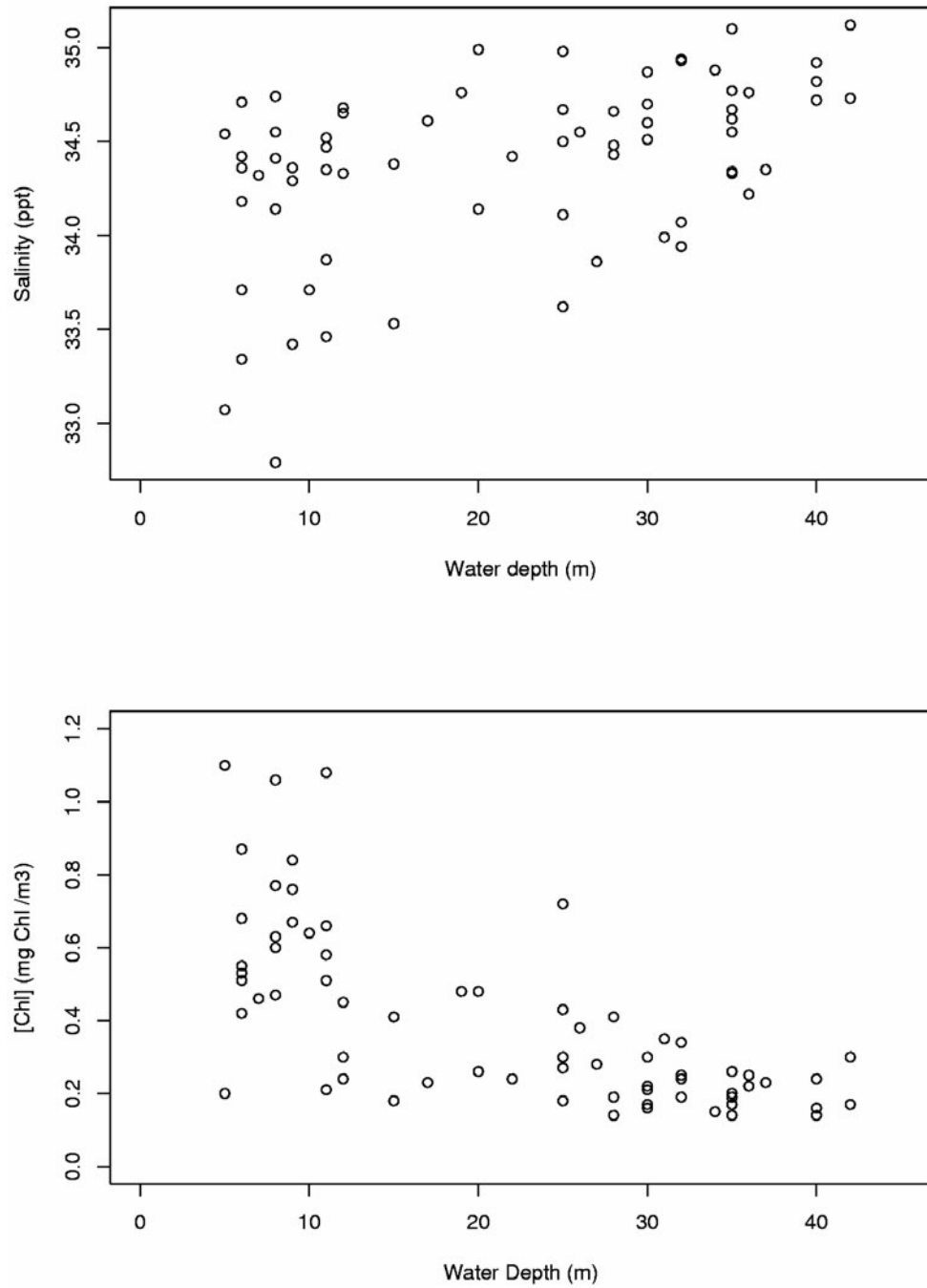


**Figure 4:** Scatterplots of the relationships between salinity and sea-floor depth (upper panel) and near-surface chlorophyll and depth (lower panel).

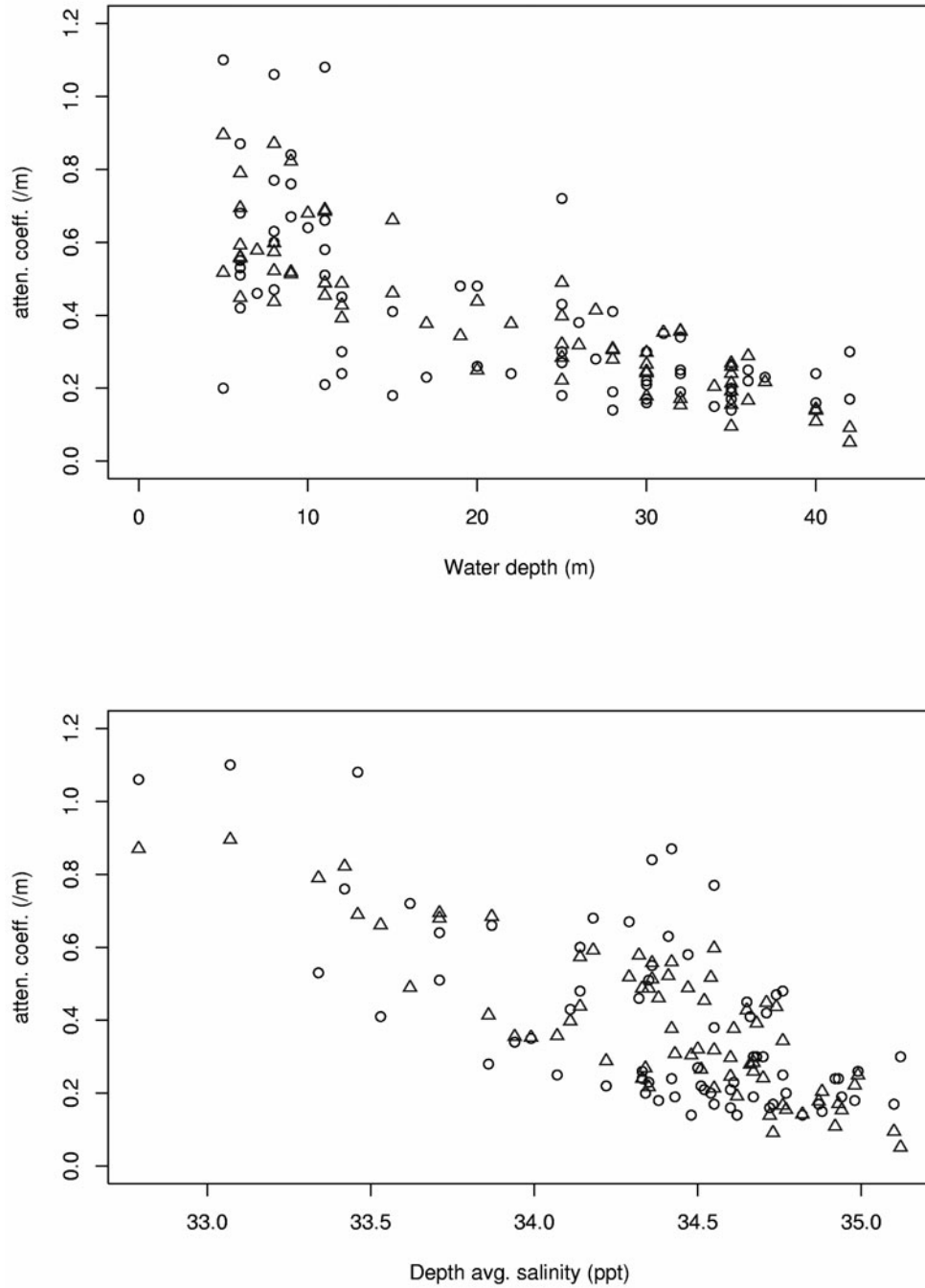


**Figure 5:** Comparison of measured (black, circle) and predicted (blue, triangle) PAR-attenuation coefficients relative to sea-floor depth (upper panel) and depth averaged salinity (lower panel).

## 3.2 Phytoplankton Modelling

### 3.2.1 Model recalibration

Even in the relatively deep and salty northern Firth, the light attenuation coefficients inferred from our analysis of the field data proved to be higher than those used in the model previously. In the southern Firth, the discrepancy was still greater.

We know of no nutrient and chlorophyll data for the extreme south of the Firth (i.e., that part of the southern Firth having water depth < 5 m, the area of interest in this study). There is however, a large body of data for the northern Firth. Thus, after incorporating the new light attenuation model, it quickly became apparent that the model was producing implausibly low phytoplankton concentrations in the northern Firth using the previous parameterisation. Whilst a formal calibration/verification exercise was beyond the scope of this contract, it was clearly necessary to undertake an informal reparameterisation exercise. The goal was not to reproduce the precise characteristics of any one data-set, but rather to obtain a parameterisation that enabled the model to perform in a manner similar to that which its predecessor (i.e., the one lacking the empirical description of light attenuation) had for the May 2003 period (refer to Appendix B of Broekhuizen, Oldman et al. (2005)). Within the available time, we were only moderately successful at achieving this (Figure 6). Nonetheless, it seems likely that the revised model (including the bug fixes alluded to in the Introduction), the revised description of light attenuation, and the revised parameterisation) is performing better than was achieved in Broekhuizen, Oldman et al. (2005). Whilst we have not made a comparison with the field data as part of this recalibration, Broekhuizen, Oldman et al. (2005) concluded that, in the region of Wilson Bay (NW Firth of Thames), their model was: (a) over-predicting the magnitude of the nearshore/offshore decline in phytoplankton biomass, (b) under-predicting the net accrual of diatoms, (c) predicting a slow decline of phytoflagellates. Each of these characteristics is less evident in the results stemming from the revised model.

Old model, old param.

Revised model, new param.

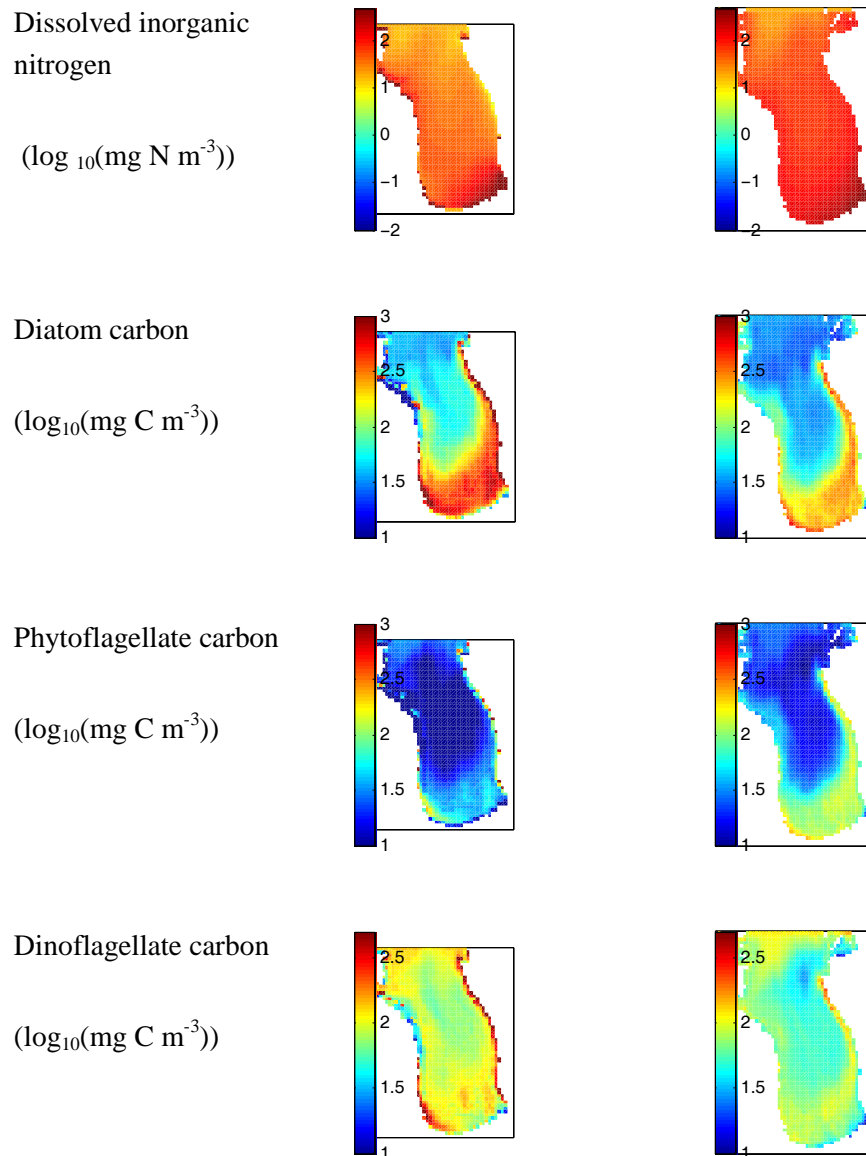


**Figure 6:** Comparison of the simulated time-and depth-averaged concentrations of dissolved inorganic nitrogen, diatom carbon, phytoplagellate carbon and dinoflagellated carbon stemming from Broekhuizen & Oldman (2005) of the model and the revised and recalibrated version of the model (right-hand figures). The colour-scale is indicative of  $\log_{10}(\text{mass m}^{-3})$ . Note that the spatial domain used for the revised version of the model extends 10 grid-cells (7.5 km) further into the Hauraki Gulf (further ‘northward’). Results are for the May 2003 period.

Given that it is the description of light attenuation that has been modified following the analysis of the field data, we chose to recalibrate the model by modifying the parameters governing the light-dependence of phytoplanktonic photosynthesis (Table

1). For all three taxa, we have substantially increased the magnitude of the initial-slope of the photosynthesis/irradiance curve (i.e., the slope at zero irradiance). We have also reduced the respective maximum weight-specific photosynthetic rates. Whilst the (recalibrated) maximum weight-specific rates of photosynthesis are comfortably within the experimentally observed range, the (recalibrated) initial slopes are very much at the upper limits of laboratory observations. It is not clear whether this is indicative of a bias arising through compensation for a structural/parametric flaw elsewhere in the model, or whether it is indicative of a genuine (photoadaptive) response by the phytoplankton of the northern Firth to low ambient light-levels.

**Table 1:** The original and recalibrated values used in the model.

Characteristic	Units	Diatoms	Diatoms	Phytofl.	Phytofl.	Dinofl.	Dinofl.
		(original)	(recalib.)	(original)	(recalib.)	(original)	(recalib.)
Max weight-specific photosynthetic rate	mg C mg <sup>-1</sup> C d <sup>-1</sup>	2.5	2.0	2.5	2.2	1.2	1.0
Initial slope of photosynthesis / irradiance relationship. (Smith curve used)	mg C mg <sup>-1</sup> C d <sup>-1</sup> / (μE m <sup>-2</sup> s <sup>-1</sup> ) <sup>-1</sup>	0.04	0.15	0.03	0.15	0.03	0.063

### 3.2.2 Simulation results: Effects of increased nutrient loading to the southern Firth

Figures 7 – 9 illustrate the time-and-depth averaged concentrations of dissolved inorganic nitrogen and of each phytoplankton taxa for each of the three seasons for the baseline scenario, together with the changes (relative to this baseline) for the two-fold and five-fold scenarios.

Note that the colour-scales used to illustrate the relative change in the concentration of each phytoplankton taxon are identical in all plots, but that those used to illustrate the relative change in DIN concentration differ from one another.

Close comparison between the results for May 2003 (Figure 9, below) and those presented for the same month in Figure 6 reveals some differences. This is because, when the simulation with the original model was made (Figure 6, above), it was run for only 20 d. For the purposes of the nutrient loadings simulations, we ran the (revised) model for 25 days (recycling the final six days of the original hydrodynamic simulation to permit this) in order to yield a more robust long-term average. To render the two sets of simulation results (old model & new model) comparable, the images in

Figure 6 are based upon the first 20 d of simulation with the new model (cf days 5-25 in Figure 9, below).

Let us start by comparing the results from the baseline loading scenario in each of the three months. There are three especially striking features. Firstly, in the September 1999 and May 2003 simulations, the time- and depth- averaged DIN concentrations are high throughout the Firth. In contrast, during the March 2000 simulation, they are low – except very close to the river mouths in the SE Firth. To some extent, this reflects the differing initial and boundary conditions used in the latter simulation, but it transpires that simulated DIN concentrations in much of the central Firth are below those adopted as initial/boundary conditions (pale blue in central Firth versus pale green at the domain's Hauraki Gulf boundary). This implies that during this simulation nutrient uptake by phytoplankton over the course of the simulation has exceeded nutrient remineralization from suspended and benthic particulates. During the May 2003 simulations, remineralization exceeded phytoplankton uptake. During September it initially exceeded phytoplankton uptake, but later fell below uptake. Whilst not evident in the time-average, nutrient-limitation developed in parts of the Firth in the last five or so days of the simulation. Field observations suggest that average chlorophyll concentrations in the northern Firth are more likely to be high in early/mid spring than at other times of the year. Thus, the model appears to be predicting the onset of springtime population growth correctly.

The second striking feature of all three simulations is that concentrations of all three phytoplankton taxa (measured as carbon) are markedly higher in the shallower parts of the Firth. Undoubtedly, the principal driver of this is that, in deep parts of the Firth the euphotic depth (i.e., the depth to which phytoplankton can achieve net positive 24-hour averaged carbon accrual) does not extend all the way to the sea-floor (Figure 3). Thus, in deeper parts of the Firth, but not in shallow parts, near-surface carbon accrual is offset by deeper-water carbon loss. Furthermore, because the model assumes that nutrient-depleted diatoms sink, this effect is exaggerated for diatoms during the March period. For the northern Firth, the simulated concentrations of phytoplankton appear plausible, but we believe those in the southern Firth are almost certainly too high to be plausible as long-term averages. Whilst conversion to chlorophyll is imprecise (carbon to chlorophyll ratios can vary by a factor of two or more even within a species), the chlorophyll concentrations in the southern Firth (Table 1) implied by these carbon concentrations are several times greater than those inferred by extrapolating from measurements in the northern and central Firth (Figure 3, Figure 4). They are also high in comparison with the majority of chlorophyll determinations made in the Manukau harbour (Vant & Budd 1993).

The third striking feature is the scarcity of dinoflagellates relative to diatoms and phytoplankton. In part, this reflects their lower growth potential (higher weight-specific basal respiratory costs and lower weight-specific maximum photosynthetic rates), but it may also be indicative of a mis-specification of the rules governing dinoflagellate swimming behaviour. The model assumes that nutrient-stressed dinoflagellates swim downwards (deeper waters are usually richer in nutrient), but otherwise they swim upwards (surface waters have more light). The Firth of Thames has a typical 'estuarine' circulation system: "salty" (= dense) waters flow into the Firth near the bed, whilst 'fresh' (= buoyant) waters flow seaward near the surface. Thus, when ambient nutrients are plentiful (September, May), the model will tend to export any accumulation of dinoflagellates much more readily than it exports the other two taxa.

A fourth characteristic is not immediately evident from the illustrations, but is worth commenting upon. Averaged over the entire Firth, diatom and phytoplankton populations tend to accrue (at worst, be stable), whilst dinoflagellate populations tend to decline (at best, be stable) over the course of each simulation. Initially, the rates of change are high. Subsequently, these decline. This suggests that the model is moving towards a (seasonally evolving) quasi-equilibrium over the course of each simulation.

Total phytoplankton abundance tends to increase. Thus, nitrogen that is initially present in dissolved inorganic or detrital forms or subsequently supplied in these forms from the rivers, or the Hauraki Gulf, is being converted into a living form (phytoplankton). With this in mind, it is worth noting that the initial pool of benthic detritus has been specified on the basis of unpublished benthic samples collected by NIWA. Like the PAR-attenuation data, these samples have been collected in waters of at least five metres' depth. They show no obvious spatial structure. For our initial conditions, we adopted an average value, and applied this throughout the Firth. During the subsequent evolution, we have noticed that shallow-water abundances of benthic detrital nitrogen tend to decline. There are three obvious explanations: (i) our initial conditions were inappropriately high, (ii) the weight-specific remineralisation rate of the detritus is too high, or (iii) the rate of delivery of detritus to the sea-floor is too low (detrital sinking speeds too low, phytoplankton mortality rates too low). If (i) or (ii) is the case, it implies that, at least initially, the seabed is providing too much remineralized nitrogen to the water-column. This would provide the fuel for what appears to be an excessive accrual of near-shore phytoplankton.

Turning now to comparisons of the three nutrient loading scenarios: both the two-fold and five-fold scenarios induce elevated DIN concentrations in the SE Firth of Thames. In the case of the five-fold scenario, DIN-elevation is marked (approximately five-fold concentration elevations in the immediate vicinity of the mouth of the Waihou) in all three seasons, but in the case of the two-fold scenario, the elevation is barely noticeable except during the September 1999 simulation. The plume of elevated DIN

is less extensive than the plume of depressed salinity (not shown). This emphasizes that unlike salt, DIN is highly reactive. Despite the fact that DIN concentrations in the SE Firth become elevated in all three seasons, it is only in March that the phytoplankton populations also become elevated. Even in this month, the increase is only evident in the case of the diatoms and phytoflagellates. Their time-averaged standing stocks increase in approximate proportion to the increased riverine loading (namely approximately two-fold and approximately five-fold). The area over which phytoplankton concentrations are elevated is a little greater than that over which DIN concentrations are increased. Even so, the areas of markedly increased phytoplankton carbon (the 'red' areas in subplots (b) and (c) of Figure 8) extends only approximately 5-10 km from the mouth of the Waihou.

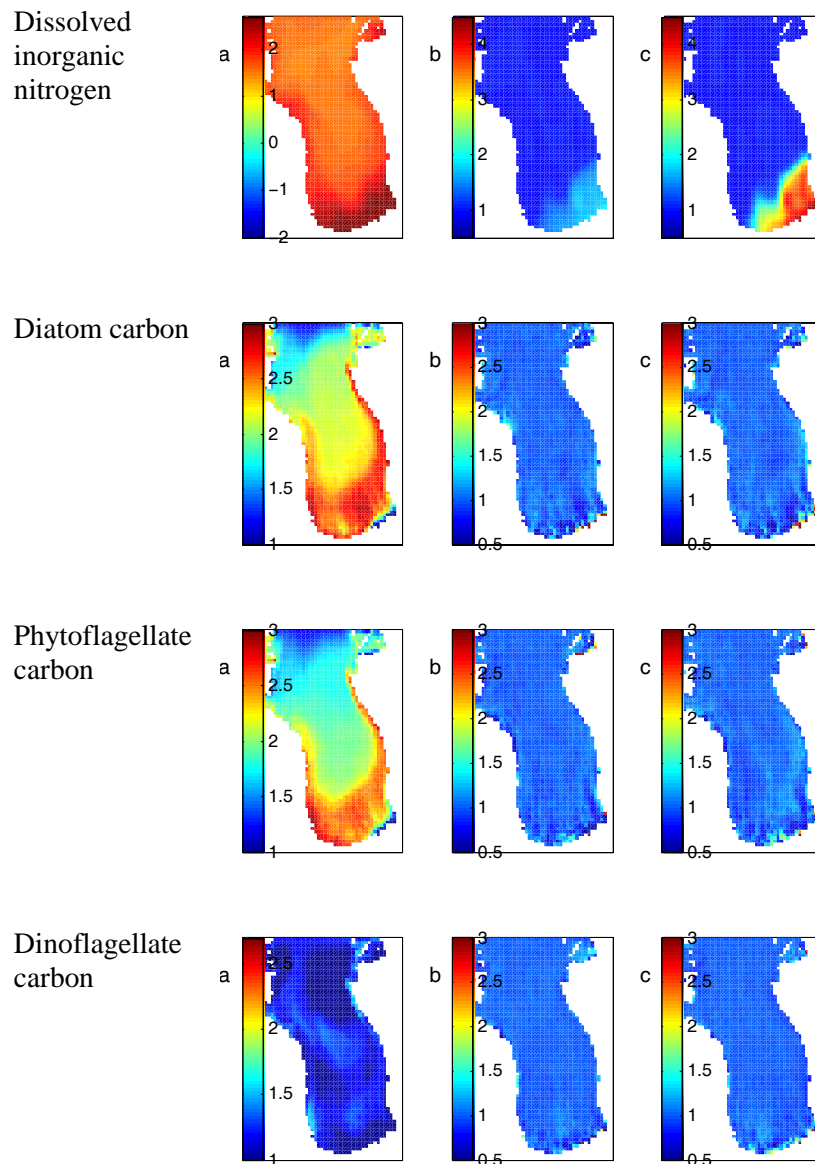


**Figure 7:** Simulated time- and depth-averaged concentrations of dissolved inorganic nitrogen, diatom, phytoplankton and dinoflagellate carbon for the **September 1999** simulation under the baseline nutrient loading scenario period (a). Also shown are the relative changes in each of these characteristics for the two-fold (b), and five-fold scenarios (c). In the concentration plots, the colour is indicative of  $\log_{10}(\text{mass m}^{-3})$ . In the ratio plots, the colour-scale is linear.

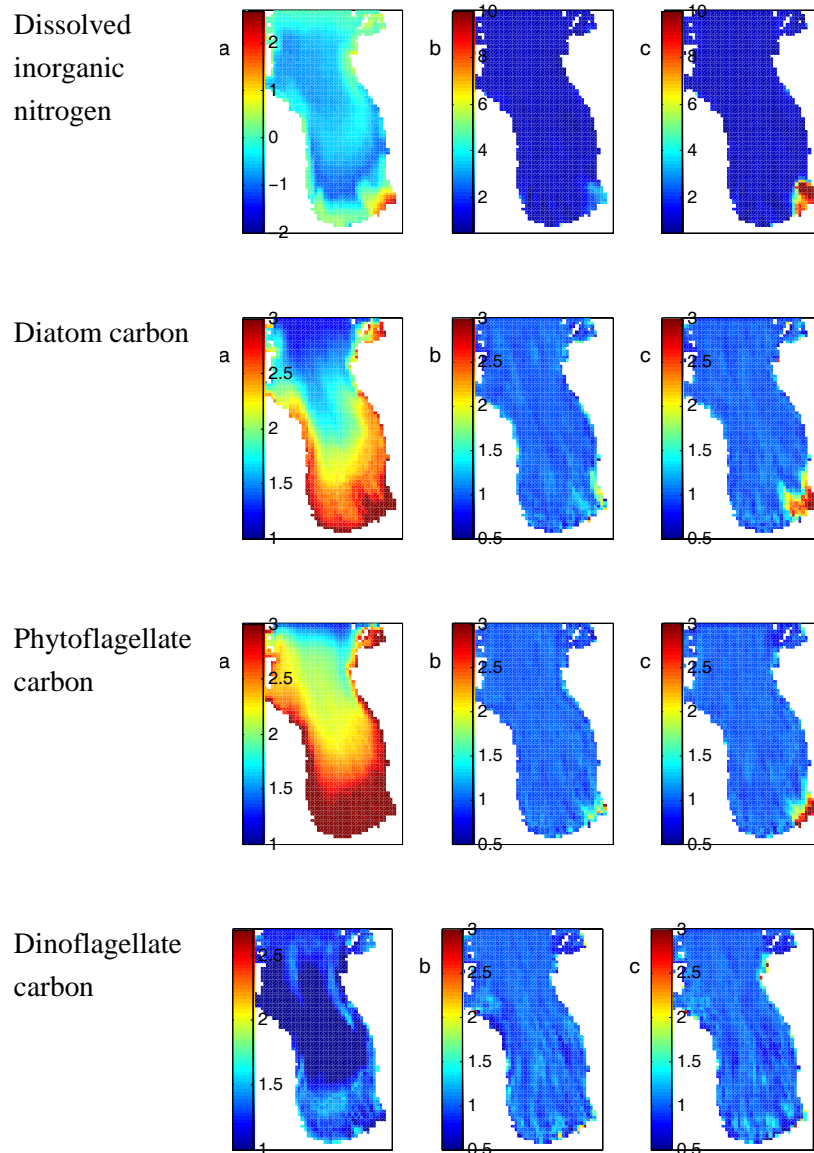


**Figure 8:** Simulated time- and depth-averaged concentrations of dissolved inorganic nitrogen, diatom, phytoplankton and dinoflagellate carbon for the **March 2000** simulation under the baseline nutrient loading scenario period (a). Also shown are the relative changes in each of these characteristics for the two-fold (b), and five-fold scenarios (c). In the concentration plots, the colour is indicative of  $\log_{10}(\text{mass m}^{-3})$ . In the ratio plots, the colour-scale is linear.

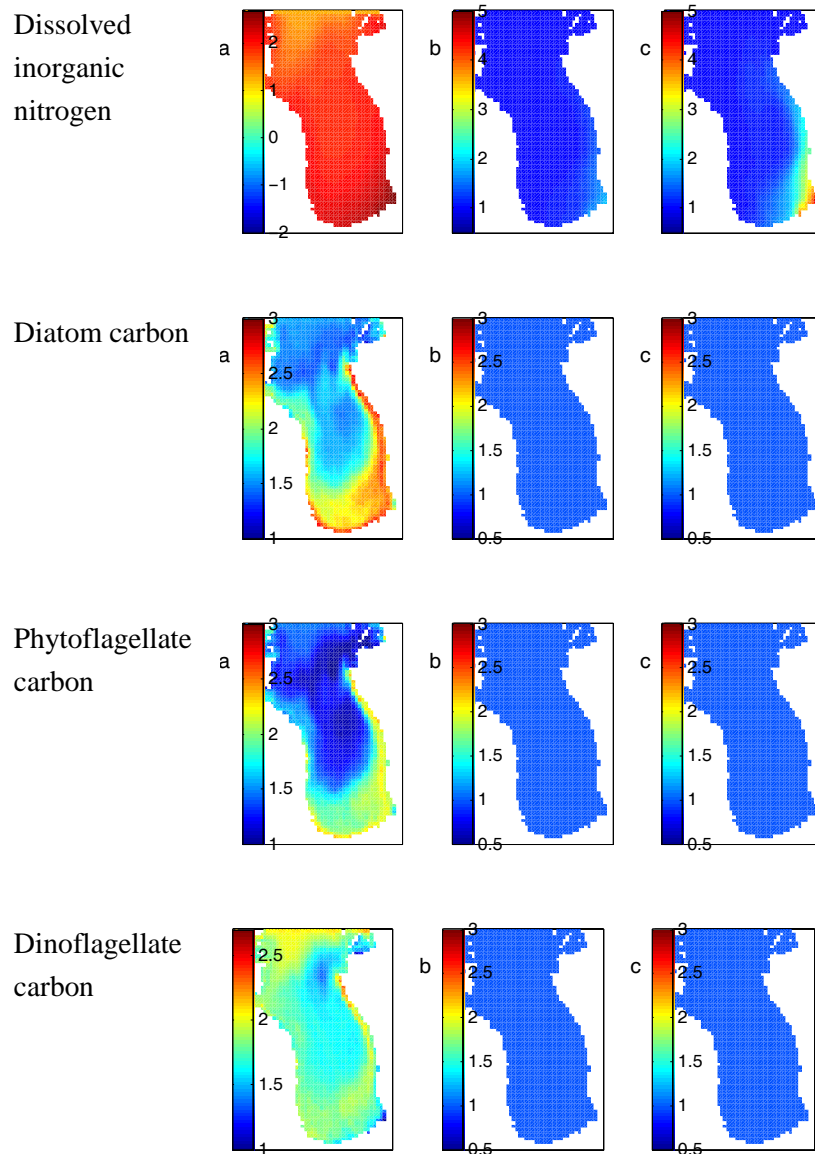


**Figure 9:** Simulated time- and depth-averaged concentrations of dissolved inorganic nitrogen, diatom, phytoplankton and dinoflagellate carbon for the **May 2003** simulation under the baseline nutrient loading scenario period (a). Also shown are the relative changes in each of these characteristics for the two-fold (b), and five-fold scenarios (c). In the concentration plots, the colour is indicative of  $\log_{10}(\text{mass m}^{-3})$ . In the ratio plots, the colour-scale is linear.

**Table 2:**

Statistical characteristics of the simulated chlorophyll concentrations in the southern Firth (<sup>4</sup>J-coordinate  $\leq 20$ , Figure 1). The mean, median and CV are calculated relative to the daily spatial arithmetic averages (i.e., a daily average over all constituent 750 x 750 m grid-cells) rather than relative to the individual daily average 750x750 grid-square concentrations. The fraction of grid-cells in which concentrations exceeded the prescribed threshold was calculated as:

$$\frac{1}{N(n-5)} \sum_{i=6}^n \sum_{j=1}^N H(\text{Chl} - \theta)$$

in which  $N$  denotes the number of water-columns having a  $J$ -coordinate  $\leq 20$  (Figure 1),  $n$  denotes the total length (days) of the simulation,  $\theta$  denotes the relevant threshold chlorophyll concentration and  $H()$  is the unit-step, or <sup>5</sup>Heaviside function. The relative grid-cell corresponds to the average fraction of the (southern) Firth that harbours a concentration in excess of the specified threshold. It is a number which integrates both the spatial- and temporal extents of 'high' chlorophyll events. It takes a value of 1.0 when all of the southern water-columns harbour chlorophyll concentrations in excess of the chosen threshold on every one of the simulated days (bar the first five days). It will take a value of zero if the threshold was never exceeded in any of the water-columns on any of the simulated days (bar the first five). As an example, let us assume that  $N=100$ ,  $n=25$  and  $\theta=10$  mg chl  $a$   $m^{-3}$ . A grid-cell-fraction of 0.2 may imply that, on each of the latter 20 days of the simulation, 20% of the water-columns harboured chlorophyll concentrations in excess of 10 mg chl  $a$   $m^{-3}$ . Alternatively, it could imply that 40% of the grid-cells harboured chlorophyll concentrations in excess of 10 mg chl  $a$   $m^{-3}$ , but that they did so on only 10 of the simulation's latter 20 days.

Season	Nutrient loading	Mean of daily spatial averages (mg Chl $a$ $m^{-3}$ )	Median of daily spatial averages (mg Chl $a$ $m^{-3}$ )	CV of daily spatial averages (-)	Fraction of grid-cells in which [chl] exceeded baseline median (-)	Fraction of grid-cells in which [chl] exceeded 10 mg chl $a$ $m^{-3}$ (-)
Sept 99	Baseline	13.74	12.39	0.70	0.404	0.454
Sept 99	Two-fold	13.60	12.35	0.70	0.399	0.452
Sept 99	Five-fold	13.62	12.27	0.70	0.397	0.450
Mar 2000	Baseline	41.99	44.60	0.27	0.259	0.995
Mar 2000	Two-fold	50.48	56.45	0.29	0.280	0.994
Mar 2000	Five-fold	64.39	84.74	0.53	0.308	0.994
May 2003	Baseline	6.48	6.83	0.30	0.410	0.197
May 2003	Two-fold	6.48	6.83	0.30	0.410	0.197
May 2003	Five-fold	6.48	6.83	0.30	0.410	0.197

<sup>4</sup> Recalling that the model has a horizontal resolution of 750 m, J-coordinate  $\leq 20$  implies that we are considering only those parts of the Firth which are  $\leq 15$  km from the domain's origin in the  $y$ -direction.

<sup>5</sup> We adopt the convention that this function is zero for chl  $a < \theta$  and one for chl  $a \geq \theta$ ; an alternative convention defines  $H(0)=0.5$ .

Table 2 provides a numerical summary of the simulations results, focussing upon the southern Firth of Thames (being that part of the Firth having a J-coordinate  $\leq 20$ , Figure 1). In September and under the baseline nutrient-loading scenario, an average of 45% of the southern Firth is predicted to have a chlorophyll concentration in excess of  $10 \text{ mg chl } a \text{ m}^{-3}$ , and 40% of the region has a chlorophyll concentration in excess of the regional median ( $12.4 \text{ mg chl } a \text{ m}^{-3}$ ). In May, the corresponding figures are 20%, 41% ( $6.8 \text{ mg chl } a \text{ m}^{-3}$ ). In March, under base-load conditions, the entire southern Firth is predicted to exhibit chlorophyll concentrations in excess of  $10 \text{ mg chl } a \text{ m}^{-3}$ ; 26% of the Firth has a concentration in excess of the regional median. Raising the inputs of riverine nutrient makes almost no difference to the fraction of the southern Firth which harbours chlorophyll concentrations in excess of  $10 \text{ mg chl } a \text{ m}^{-3}$  – in any of the seasons. Similarly, in September and May, raised nutrient inputs make little difference to the fraction of southern Firth which harbours chlorophyll concentrations in excess of the regional mean. In contrast, in March, raising the nutrient inputs drives a marked-increase in the fraction of the southern Firth which harbours chlorophyll concentrations in excess of the median.

### 3.2.3 Robustness Analysis

The biophysical model is moderately complex. The appropriate mathematical form by which to describe some of the rate-processes is uncertain. Similarly, the appropriate values for many of the parameters are only known approximately. One of the conclusions from the preceding section was that the model (loosely calibrated so as to reproduce plausible phytoplankton concentrations in the northern Firth) yields phytoplankton concentrations in the southern Firth which we believe to be implausibly high. Thus, though our contract does not stipulate that a sensitivity analysis be performed, we offer the following (very restricted) analysis. This is aimed at determining whether one of our key assumptions may be responsible for the probable over-prediction of shallow-water phytoplankton concentrations.

The reader will recall: (i) that the field data from which the empirical relationship between light attenuation and local environmental characteristics stems only from water of greater than 5 m depth – and is therefore biased towards being a measure of ‘green’ light attenuation; (ii) since Environment Waikato are most interested in how increased riverine nutrient loads might influence the shallow, southern Firth, we were forced to extrapolate the relationship into shallow water and make an assumption as to how ‘red’ light may be attenuated.

In the simulations reported within the preceding section, we assumed that the ‘green’-light attenuation coefficient equalled that inferred from the empirical attenuation relationship, and that the ‘red’-light attenuation coefficient was equal to the sum of the inferred ‘green’ attenuation coefficient and 0.32 (being the approximate difference between the pure-water attenuation coefficients of ‘red’ and ‘green’ light). This

rescaling is appropriate if, in reality, the attenuation increment (over that of pure-water) is due primarily to increased absorbance per linear vertical m (i.e., due to a broad-spectrum of coloured materials in the water). If it is instead due to increased mean path-length per vertical m (increased scattering) this rescaling will have underestimated the attenuation of red light. We suggest the following alternative as being more appropriate if scattering is the dominant cause of the increased light attenuation:

$$k_{realised}^{red} = k_{pure}^{red} \frac{k_{realised}^{green}}{k_{pure}^{green}},$$

In which  $k$  denotes an attenuation coefficient ( $m^{-1}$ ), the subscript denotes whether this applies to pure water, or to the local environmental conditions, and the superscript indicates which part of the visible spectrum it refers to. Once again, we apply clipping at  $k_{realised}^{green} = 2.0 m^{-1}$  and  $k_{realised}^{red} = 2.32 m^{-1}$ . Since  $k_{realised}^{green}$  usually exceeds  $0.2 m^{-1}$ , whilst  $k_{pure}^{green} = 0.08 m^{-1}$  and  $k_{pure}^{red} = 0.4 m^{-1}$ , this implies that  $k_{realised}^{red}$  will be substantially greater with this alternative model than it was previously. Furthermore, the absolute increment will now increase as depth shallows (or salinity falls). With the previous formulation, the red-light increment was constant and clipping of ‘red’ light attenuation was rarely invoked. With this formulation, the increment is not spatially invariant, and clipping occurs more frequently in shallow water. As we have discussed previously, even in pure-water ‘red’ light is attenuated much more rapidly than ‘green’ light. Thus, we anticipate that this formulation change will be dynamically more important in shallow parts of the Firth (where water-column primary production will occur under the influence of both ‘red’ and green’ light) than in deeper parts of the Firth (where a substantial part of the production occurs ‘deep’ in the water-column under the influence of only ‘green’ light). Nonetheless, even in offshore areas, we do anticipate some reduction in productivity. Despite this, we will not endeavour to recalibrate any of the other parameters in the model (as may be required to maintain similar standing stocks in the northern Firth).

It transpires that adoption of the alternative light attenuation model leads to only very slight reductions in phytoplankton standing stock (Figure 10). Whilst the temptation is, therefore, to conclude that the model is insensitive to the magnitude of PAR attenuation in shallow water, we caution that this may well be due to the influence of our decision to ‘clip’ extrapolated ‘red-light’ attenuation coefficients at approximately  $2.4 m^{-1}$ . With the alternative model for deriving ‘red-light’ attenuation, the extrapolated-but-not-yet-clipped ‘red’-light attenuation coefficient frequently exceeds this value in shallow waters. This demonstrates that our findings are not sensitive to the scaling between ‘red’-light and ‘green’-light attenuation coefficients.

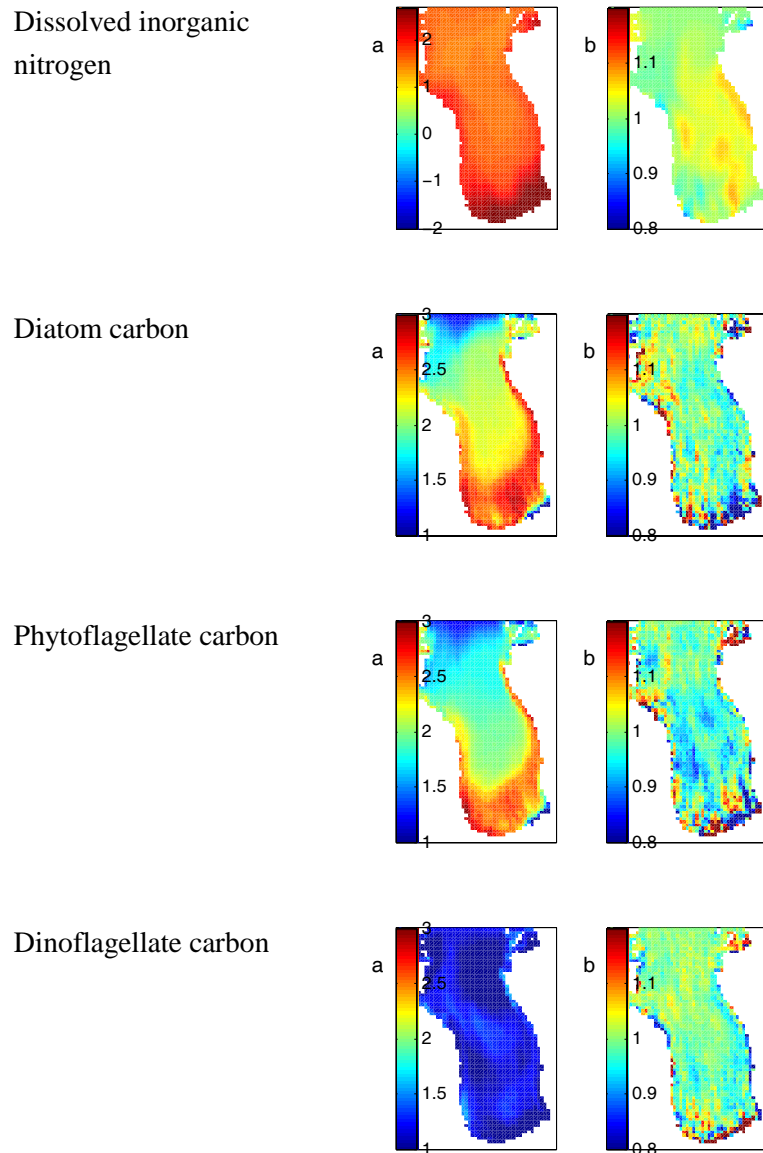


**Figure 10:** Comparison of time- and depth-averaged simulation results for the September 1999 simulation using the original means of calculating a ‘red’-light attenuation coefficient; right-hand column relative difference when the alternative means of calculating the attenuation coefficient is used. In the concentration plots (left-hand column), the colour is indicative of  $\log_{10}(\text{mass m}^{-3})$ . In the ratio plots (right-hand column), the colour-scale is linear.

## 4. Discussion

### 4.1 Plausibility of results: shallow water processes absent from the model

Up until this investigation, applications of the model had focussed upon the northern and central Firth of Thames. Comparatively little attention had been focussed upon its performance in very shallow parts of the Firth. Whilst previous experience causes us to believe that the model (particularly this recalibrated model) is reproducing phytoplankton concentrations in the northern Firth moderately well, our experience during this investigation leaves us less satisfied that this is proving to be the case for very shallow parts of the Firth.

We have remarked upon the marked increase in simulated time-average phytoplankton abundance as one moves from deeper parts of the Firth to shallow parts. There is certainly evidence in our field data that shallow-water phytoplankton abundances are genuinely higher than those found in deeper water (e.g., Figure 4). Nonetheless, the simulated concentrations in the southern Firth (frequently in excess of  $\text{mg chl } a \text{ m}^{-3}$  assuming C : chl ratios of approx. 50:1) are several times greater than those implied by an informal, visual extrapolation of the depth/chl scatter-plot relationship (Figure 4) into water of less than 5 m depth. Furthermore, as already noted, we know of no reports (anecdotal or otherwise) of algal blooms in the southern Firth – suggesting that chlorophyll concentrations rarely, if ever exceed approximately  $10 \text{ mg Chl } a \text{ m}^{-3}$ . Set against this, we note that Williamson et al. (2003) report that during the summer months, chlorophyll concentrations in the turbid, shallow, nutrient-rich north-eastern Manukau often exceed  $10 \text{ mg Chl } a \text{ m}^{-3}$  (sometimes reaching more than  $60 \text{ mg Chl } a \text{ m}^{-3}$ ). During the remainder of the year, they are usually in the range  $2\text{-}10 \text{ mg Chl } a \text{ m}^{-3}$ . The conflicting evidence stemming from our extrapolation of the northern/central Firth data and the Manukau data make it difficult to know whether the biophysical model is performing as well in the southern Firth as we believe it to be in the northern Firth. Our tentative suggestion is that the chlorophyll concentrations inferred from the model are more likely to be typical of short-term, localised blooms than large-scale, seasonal averages. As such, the model's forecasts of the response to nutrient-loading might be regarded as being 'worst-case'.

One can speculate that though our model performs moderately well in deeper parts of the Firth, it lacks adequate descriptions of several processes that may be important in shallow waters. There are three deficiencies that may be especially important. Two relate to phytoplankton mortality, and one to phytoplankton productivity.

The model has no explicit representation of phytoplankton losses to the community of benthic filter-feeders. Whilst the model's mortality term purports to represent the sum

of mortality due to all causes other than ‘starvation’ (i.e., consumption by zooplankton and benthic filter-feeders, death caused by pathogens etc.). Nonetheless, because it is spatially invariant, it is unlikely to provide a good description of losses to benthic filter-feeders. Expressed on a water-column averaged basis, it is clear that the weight-specific phytoplankton mortality induced by a given population of benthic filter-feeders will decline inversely with depth. The filtration rates of most benthic filter-feeding species are unknown, but an adult Greenshell mussel (*Perna canaliculis*) can filter in excess of 100 L d<sup>-1</sup> (Hawkins et al. 1999) and can attain densities of 100s of individuals m<sup>-2</sup> in natural beds. Adult Horse-mussel (*Atrina zelandica*) will filter a few 10s of L d<sup>-1</sup>, and can attain densities of approximately 100 of individuals m<sup>-2</sup> (Ellis et al. 2002; Green et al. 1998). For the Manukau harbour, McBride et al. (1993) estimated that benthic filter-feeders filter approximately 1 m<sup>3</sup> of water m<sup>-2</sup> of seabed d<sup>-1</sup>. Averaging over the water-column depth, this implies that phytoplankton mortality due to benthic filter-feeders amounts to 100% d<sup>-1</sup> if the water-column is 1 m deep, but only 10% d<sup>-1</sup> if it is 10 m deep. Bivalve densities in the inter-tidal southern Firth of Thames range from approximately 10 m<sup>-2</sup> to several hundred m<sup>-2</sup> and filter-feeding species become relatively more abundant towards the low-tide mark (Brownell 2004). We infer that benthic filtration rates are likely to be large in the lower inter-tidal zone, and probably also in the shallow sub-tidal zone. We know of no published records for the sub-tidal southern Firth – though NIWA does hold some unprocessed core-sample material (M. Morrison, NIWA *pers. comm.* 27 October, 2005).

In addition to benthic-filter-feeders, there is a second mechanism which may lead to greater phytoplankton mortality in very shallow (more specifically, inter-tidal) regions. On the falling tide, it is possible that some of the phytoplankton cells become stranded and subsequently desiccate or become bleached in the bright sunlight. We know of no data by which to quantify this effect. It is not a part of the present biological model. Indeed, there is no inter-tidal zone in the hydrodynamic model which underpins our biological simulations. At the time that it was developed, attention was focussed upon the northern Firth and the developers of the hydrodynamic model chose to <sup>6</sup>artificially deepen the shallowest parts of the Firth in order to eliminate the inter-tidal regions – thereby rendering the hydrodynamic model more numerically tractable. .

If, as seems likely, per-capita phytoplankton productivity is greater in shallow parts of the Firth, it is probable that at least a fraction of the additional production will manifest itself as increased grazer or pathogen biomass rather than increased phytoplankton biomass. This being so, it is probable the weight-specific mortality rate

---

<sup>6</sup> It is also worth noting that, because of this artificial deepening, the resultant extrapolated diffuse light attenuation coefficients will have been lower than they would otherwise have been. We suspect that this is dynamically unimportant. Even in shallow water, the extrapolated coefficient becomes ‘large’ only when the water is relatively fresh. Furthermore, the effects of artificially reduced attenuation coefficient are somewhat offset by the artificially increased water-column depth.

would be higher in the shallower parts of the Firth – except near river mouths. There, we anticipate that mortality due to zooplankton will be reduced. Zooplankton exhibit lower potential demographic growth rates than phytoplankton, yet are equally liable to advective export from the vicinity of river-mouths. Thus, their realised population density will be reduced disproportionately relative to that of the phytoplankton (Speirs & Gurney 2001). Even if we disregard the possibility of increased predator-induced losses, it is possible that the weight-specific mortality rates of phytoplankton are higher in the inter-tidal zones than elsewhere – due to desiccation and sunlight-induced bleaching of stranded phytoplankters.

The third deficiency relates to the absence of any description of the photoadaptation and photoinhibition responses that phytoplankton demonstrate. Photoadaptation refers to the tendency of phytoplankton to regulate the nature of their photosynthetic ‘machinery’ in response to ambient light intensities (e.g., increasing the cell-specific chlorophyll content, and increasing the size of the chlorophyll antenna per synthesis site) in response to low light intensities. The corollary of this behaviour is that we would expect that phytoplankton in very shallow water will tend to require higher light-intensities than phytoplankton (deep) within deeper water. Since (i), our model has no representation of this mechanism, and (ii) we have chosen to calibrate the photosynthetic parameters relative to expectations of its behaviour in deep parts of the Firth, we may have caused the model to over-predict phytoplankton production in shallow parts of the Firth. Photoinhibition refers to the tendency of the photosynthetic machinery to become damaged (hence, less productive) when exposed to light intensities which are persistently higher than the machinery is adapted to. Whilst photoinhibition is a transient phenomenon (recovery occurs as the system adapts to higher light intensities), phytoplankton are not infinitely adaptable, and may be incapable of fully adapting to the very high light levels that our model suggests occurs very close to the sea-surface. If this is the case, it too points to our model over-predicting shallow-water phytoplankton production.

Other, perhaps less likely, means by which phytoplankton demographic growth may be suppressed in shallow water relative to that in deep-water include: (a) greater potential for entrapment on the sea-floor (burial by sediment or capture on biogenic mucilage), and (during periods of nutrient limitation) pre-emptive consumption of nutrients emerging from the sea-bed by benthic algae (which will be much less abundant in deeper water).

There is an important distinction to be drawn between so-called ‘top-down’ and ‘bottom-up’ limits upon phytoplankton abundance. A trophic group is said to be ‘bottom-up’ controlled when its abundance is limited by resource availability (e.g., nutrients or irradiance). It is said to be ‘top-down’ controlled if its abundance is

limited by grazing-pressure. In a bottom-up controlled system, addition of more of the limiting resource permits the trophic group in question to achieve greater biomass – but can also push it towards top-down control (Rosenzweig 1971). Whilst phytoplankton are generally considered to be ‘bottom-up’ controlled, the preceding discussion suggests that our model may under-estimate the magnitude of top-down (grazing) influences. Since the model assumes that the grazer-population has no numerical, or functional response to phytoplankton concentration (i.e., the weight-specific mortality induced by grazers is independent of phytoplankton concentration), an expansion of the phytoplankton population can only be brought to a standstill by nutrient-limitation, or ‘self-shading’ (shading of phytoplankton deep in the water-column by those above). Nutrient delivery at the river-mouths is independent of the phytoplankton concentrations immediately outside the mouth. Thus, nutrient-limitation cannot arise in the immediate vicinity of the nutrient-laden river-mouths in the SE Firth. Equally, self-shading only becomes significant at very high phytoplankton abundances. Thus, as the model is formulated at present, it is inevitable that increased nutrient loading (into a system that is otherwise nutrient-limited) will yield elevated chlorophyll concentrations in the immediate vicinity of the river-mouth. The more interesting question is: “over what radius from the river-mouth will this enhancement be evident?”. The model suggests that under the five-fold enhancement scenario, the radius will be 5–10 km.

#### **4.2 Caveats: other simplifying assumptions**

Whilst the preceding section refers to generic structural issues, there are some additional assumptions related to the manner in which we have implemented the two elevated loading scenarios. These include:

- Increased nitrogen loading will not modify nutrient-remineralization processes (including the fraction of benthic PON remineralization flux which is lost from the water-column as denitrified  $N_2$ ). If organic loadings were to become sufficiently high, it is possible that denitrification would cease. All of the remineralized nitrogen would then be returned to the water-column. One might then anticipate a still greater response by phytoplankton. In this context, it should be noted that even at the Firth-scale, denitrification rates are uncertain. Giles (2001) estimated that denitrification amounts to approximately 14% of the remineralization flux, but Zeldis (2005) estimated that nitrogen passes around the primary production / degradation / remineralization cycle only three times prior to being remineralized. This suggests that denitrification may divert substantially more than 14% of the benthic remineralization flux into  $N_2$ . In the shallow parts of the Firth, benthic remineralization is particularly important. If the initial benthic pool is too large, and/or the denitrification fraction is too low, N-limitation will have been under-predicted and phytoplankton populations over-predicted.

- The numerical response of benthic or planktonic grazers is such that they continue to impose exactly the same weight-specific mortality upon the phytoplankton. In the preceding section, we remarked upon the possibility that a numerical response by grazers could result in southern Firth phytoplankton suffering a greater weight-specific grazing mortality than those in the north. A similar process could occur at a finer scale – with those in the river-plumes suffering more mortality than those outside the plumes. If so, this would dampen the biomass response exhibited by the phytoplankton.

### 4.3 Seasonality of response to loading

With respect to the question which generated this investigation, our key conclusion is that elevated riverine nutrient loadings induced an increase in phytoplankton concentrations in only one of the three seasons that we examined. The reason for this is that, in the model, phytoplankton growth is limited by ambient DIN concentrations during the March simulation, but not during the May or September simulations. During these latter months, lower irradiance (May) or water-temperatures (September) limit phytoplankton growth rates to a greater degree than do ambient DIN concentrations. Indeed, realised growth rates are such that nitrogen remineralization (at least) balances the phytoplankton nitrogen consumption rates. Thus, additional nitrogen is of no consequence to the phytoplankton in the latter two months.

We acknowledge that the model may be over-predicting phytoplankton concentrations in the southern Firth (therefore, overpredicting the likelihood of nutrient limitation). Nonetheless, from a management perspective, the critical ancillary question is: over which months of the year do ambient nitrogen concentrations limit phytoplankton growth rates? Since we have neither nutrient- nor chlorophyll data for the southern Firth, we will begin by discussing the northern Firth – where we do have data. There, it seems that along-shore wind-stress (which influences the strength of upwelling at the continental shelf), and wind-strength (influencing the strength of mixing across the nutricline) are the dominant determinants of the concentration of dissolved inorganic nitrogen (Zeldis 2004; Zeldis et al. 2005). Nonetheless, there is a weak seasonal signal, with DIN concentrations tending to be higher during the late autumn – early spring period.

Current-flow patterns are such that we anticipate the southern Firth will be less influenced (than the Firth as a whole) by upwelling on the coastal shelf. Intuition, and our simulation results both indicate that riverine inputs do influence the nutrient concentrations in the southern Firth. Monthly average river-flows are highest in the autumn months (and nitrate concentrations in this river water also tend to be a little

higher in the winter). Thus, we suspect that nutrient concentrations in the southern Firth will show a clearer seasonal cycle than those in the northern Firth (being higher in winter). In the September simulation, nutrient-limitation became evident in some parts of the Firth in the latter days of the simulation. Had the simulation been run for longer, or had we chosen lower initial conditions for the N-content of the Firth (notably, benthic detrital nitrogen), this limitation would have become more evident. We therefore believe that our finding of no significant phytoplankton response to increased nutrient loading in September is likely to be sensitive to initial conditions, model parameters and inter-annual variations in weather conditions in late winter and early/mid spring. We conclude that elevated riverine nutrient loading is most likely to influence southern Firth phytoplankton standing stocks only over the period<sup>7</sup> September/October - April.

#### 4.4 Robustness of conclusions

Our conclusions regarding seasonal window during which elevated nutrient loading may influence phytoplankton accrual are dependent upon two inter-related issues:

- a) that phytoplankton cell-specific growth can become sufficiently rapid that it induces nutrient draw-down (i.e., at least for some periods, water temperatures and irradiance are plentiful);
- b) that demographic losses (export of cells from the locality with out a accompanying import and mortality to grazers, pathogens etc.) are sufficiently low that the positive cell-specific carbon-accrual implied by (a) is translated into prolonged population growth.

Whilst phytoplankton growth is influenced by water-temperature, we consider it unlikely that the hydrodynamic model will be producing water-temperatures which are sufficiently erroneous (i.e., several degrees in error) to drive ‘significant’ changes in the forecaste demographics. Similarly, the irradiance model uses a standard formulation for clear-sky irradiance (as a function of latitude, time of year and time of day). PAR losses to cloud-cover are not accounted for, but the fact that shallow-water phytoplankton concentrations have proven to be insensitive to marked changes in within-water column PAR attenuation indicates that cloud-cover effects are likely to be negligible. Thus, we believe that the environmental conditions governing individual phytoplanktonic growth are adequately represented. Similarly, through using a model which explicitly represents the three physiologically very distinct divisions amongst the phytoplankton, we have taken some steps towards reducing

---

<sup>7</sup> In deeper parts of the Firth, short-term stabilisation of the water-column, followed by nutrient-drawdown within the surface waters may occur even in winter. In such situations, the associated algal bloom would be larger were the nitrogen content of the water column (pre-stabilisation) greater.

uncertainties associated with parameterising growth responses. We suggest that, with the possible exception of the parameter governing the initial slope of the photosynthesis/irradiance curve, the parameters governing physiology would have to be modified to an implausible degree before individual phytoplankton would be incapable of exhibiting rapid, positive net growth in shallow parts of the Firth.

As with temperature, we believe that it is unlikely that the hydrodynamic model could be producing residual currents which are so much in error that changed immigration/emigration could significantly modify phytoplankton demography in the southern Firth. In contrast, as discussed previously, there is ample scope for the assumed phytoplankton mortalities to be too low.

Overall, we believe that our simulations produce a plausible indication of the ‘worst-case’ demographic response of the phytoplankton population to elevated nutrient delivery into the south-eastern Firth of Thames. We suspect, however, that such high (baseline scenario) phytoplankton concentrations would rarely be achieved.

#### 4.5 Further work

The performance of the biophysical model (and the hydrodynamic model) in the very shallow southern Firth have not been closely examined previously (this issue was discussed in NIWA’s original project proposal). Whilst we believe that our conclusions are robust ‘worst-case’ predictions, we have offered several reasons as to why the average standing stocks of phytoplankton in the very shallow parts of the Firth may be over-predicted. Based upon our analysis of the field-data and our modelling results, we suggest that the following additional work would be required to if better forecasts of ‘run-of-the-mill’ enhancement are to be made.

- a) Measurement of chlorophyll concentrations in the southern Firth of Thames (inside 5 m depth contour). This would quickly reveal whether the 10 mg chl  $a\ m^{-3}$  threshold is already being exceeded and permit the model to be better calibrated to the area of interest in this application.
- b) An investigation of the model’s sensitivity to: (i) the capping-threshold applied to the PAR-attenuation coefficient, and (ii) perturbations to our empirical predictor of the diffuse-light attenuation coefficient (from water depth and salinity). This would determine whether further measurements of PAR attenuation are required (in water of < 5 m depth).

- c) If warranted by (b), collection of PAR attenuation data from water inside the 5 m depth contour. This would reduce the doubts associated with having to extrapolate our empirical relationship, and verify our decision to cap the attenuation coefficient at  $2 \text{ m}^{-1}$  – as noted previously higher values than this have been reported in some estuaries (Vant 1991).
  
- d) A (numerical) investigation of the model's sensitivity to the introduction of mortality term related to the activities of benthic filter-feeders. In particular, this would enable us to determine whether the forecast magnitudes and radii of enhancement are sensitive to the 'baseline' standing stock of phytoplankton in the southern Firth. It would also provide an indication of whether an analysis of archived core-sample material and/or field-surveys may be warranted.
  
- e) If warranted by (d), analysis of the nature (taxonomy, abundance and size-structure) of the shallow-water, sub-tidal, benthic filter-feeder community. This would enable us to infer a realistic benthic filtration rate.
  
- f) Collection of benthic particulate organic nitrogen and benthic dissolved organic nitrogen samples from water shallower than 5 m depth together with work directed at better quantifying the processes governing rates of remineralization and denitrification in benthic sediments. During periods of nutrient-limitation, the rate of benthic nutrient regeneration may prove a key determinant of realised phytoplankton stocks. If so, the relative magnitudes of the nutrient supply through benthic regeneration and diffusive/advective delivery of riverine nutrient will influence the radius to which phytoplankton stocks may be enhanced by increased riverine nutrient loads.

## 5. Acknowledgements

The hydrodynamic simulation results that have been used in this project were generated in two earlier ones. One was funded by Environment Waikato, Auckland Regional Council and the Western Firth Mussel Farming Consortium. The other was funded by Environment Waikato and the Auckland Regional Council. We thank these organisations for granting us permission to use the results from these earlier projects within this one.

## 6. References

- Broekhuizen, N. (1999). Simulating motile algae using a mixed Eulerian-Lagrangian approach: does motility promote dinoflagellate persistence or co-existence with diatoms? *Journal of Plankton Research* 21(7): 1191-1216.
- Broekhuizen, N.; Oldman, J. (2002). Between-individual variations modify phytoplankton dynamics. *Water & Atmosphere* 10(4): 10-12.
- Broekhuizen, N.; Oldman, J.; Image, K.; Gall, M.; Zeldis, J. (2005). Verification of plankton depletion models against the Wilson Bay synoptic survey data. *Report No. HAM2005-02*. 65 p.
- Broekhuizen, N.; Zeldis, J.; Stephens, S.A.; Oldman, J.W.; Ross, A.H.; Ren, J.; James, M.R. (2002). Factors related to the sustainability of shellfish aquaculture operations in the Firth of Thames: a preliminary analysis. *Report No. EVW02243*. 106 p.
- Brownell, W. (2004). Muddy Feet. Firth of Thames Ramsar site update 2004. *Report No. 1*. 203 p.
- Close, M.E.; Davies-Colley, R.J. (1990). Baseflow water chemistry in New Zealand rivers. 1. Characterisation. *New Zealand Journal of Marine and Freshwater Research* 24: 319-341.
- Ellis, J.; Cummings, J.; Hewitt, J.; Thrush, S.; Norkko, A. (2002). Determining effects of suspended sediment on condition of a suspension feeding bivalve (*Atrina zelandica*): results of a survey and a field transplant experiment. *Journal of Experimental Marine Biology & Ecology* 267: 147-174.
- Giles, H. (2001). Modelling Denitrification in Continental Shelf Sediments. M.Sc. University of Waikato, Hamilton. 110 p.
- Green, M.O.; Hewitt, J.E.; Thrush, S.F. (1998). Seabed drag coefficient over natural beds of horse mussels (*Atrina zelandica*). *Journal of Marine Research* 56: 613-637.
- Hall, J.A.; Safi, K.A.; James, M.R.; Weatherhead, M.A. (in review). Microbial assemblage dynamics during the spring - summer transition on the northeast continental shelf of New Zealand. *New Zealand Journal of Marine and Freshwater Research*.
- Hawkins, A.J.S.; James, M.R.; Hickman, R.W.; Hatton, S.; Weatherhead, M. (1999). Modelling of suspension-feeding and growth in the green-lipped mussel *Perna canaliculus* exposed to natural and experimental variations of seston availability in the Marlborough Sounds, New Zealand. *Marine Ecology Progress Series* 191: 217-232.
- Kirk, J.T.O. (1983). Light and photosynthesis in aquatic ecosystems. Cambridge University Press, Cambridge, U.K. p.
- McBride, G.B.; Vant, W.N.; Cloern, J.E.; Liley, J.B. (1993). Development of a model of phytoplankton blooms in Manukau Harbour. *Report No.* p.
- Oldman, J.; Hong, J.; Stephens, S. (2005). Verification of the Firth of Thames hydrodynamic model. *Report No. HAM2005-127 (ARC05243)*. 69 p.
- Rosenzweig, M. (1971). Paradox of enrichment: destabilization of exploitation ecosystems in ecological time. *Science* 171: 385-387.

- Speirs, D.C.; Gurney, W.S.C. (2001). Population persistence in rivers and estuaries. *Ecology* 82(5): 1219-1237.
- Stephens, S.A.; Broekhuizen, N. (2003). Ecological sustainability assesment for the Firth of Thames: Task 1 - Hydrodynamic modelling. *Report No. HAM2003-113*. 35 p.
- Vant, W.N. (1991). Underwater light in the northern Manukau Harbour, New Zealand. *Estuarine, Coastal and Shelf Science* 33: 291-307.
- Vant, W.N.; Budd, R.G. (1993). Phytoplankton photosynthesis and growth in contrasting regions of Manukau Harbour, New Zealand. *New Zealand Journal of Marine and Freshwater Research* 27: 295-307.
- Williamson, B.; Lewis, G.; Mills, G.; Vant, B. (2003). Contaminants on the coast. *In: Roff, J.R.; Nichol, S.L.; Rouse, H.L. (eds). The New Zealand Coast*, pp. 312. Dunmore Press and Whitireia Publishing, Palmerston North, Wellington.
- Zeldis, J.R. (2003). Voyage report KAH0303. *Report No.* p.
- Zeldis, J.R. (2004). New and remineralised nutrient supply and ecosystem metabolism on the northeastern New Zealand continental shelf. *Continental Shelf Research* 24: 563-581.
- Zeldis, J.R. (2005). Magnitudes of natural and mussel-farm derived fluxes of carbon and nitrogen in the Firth of Thames. *Report No. CHC2005-048*. Environment Waikato Technical Report 2005/30. 42 p.
- Zeldis, J.R.; Oldman, J.; Ballara, S.L.; Richards, L.A. (2005). Physical fluxes, pelagic ecosystem structure, and larval fish survival in Hauraki Gulf, New Zealand. *Canadian Journal of Fisheries and Aquatic Science* 62: 593-610  
doi:510.1139/F1104-1209.

## 7. Appendix A. Point source nutrient loads (baseline scenario)

The ensuing tables list the flow-rates and nutrient concentrations used in the baseline scenarios. The flows are monthly averages, and the nutrient concentrations are flow-weighted averages (nitrogen), or derived from scarce grab-samples (DRSi). For the rivers, the flow and nitrogen data were provided by Environment Waikato. The DRSi value stems from Close & Davies-Colley (1990). The data for the Thames Sewage discharge were also provided by Environment Waikato. They stem from the Assessment of Environmental Effects report for the discharge.

The monitoring data for the rivers measures three nitrogen components: nitrate-N, ammoniacal-N, and total N. For the purposes of modelling, nitrate-N and ammoniacal N have been combined to correspond with the model's DIN. Total nitrogen measures not only dissolved inorganic N, but also dissolved and particulate organic N. It is not clear whether all of this organic N is bio-available, but in consultation with Environment Waikato, we opted to make a 'worst-case' assumption (in terms of total bioavailable N-loading to the Firth). Thus, we assume that all of the organic N is bioavailable. Initially, it enters the model's 'pelagic particulate organic nitrogen pool' (PON). POC is calculated from PON assuming a Redfield-like C:N ratio. The model assumes that pelagic organic detritus sinks. Thus, much of the riverine organic N settles near the river mouths. In the model, both pelagic and benthic particulate matter remineralize at a weight-specific rate of  $0.01 \text{ d}^{-1}$ , but 14% of the N-flux stemming from benthic remineralization is assumed to be lost from the system as  $\text{N}_2$ .

For modelling purposes, the values quoted in the tables were assumed to hold at the mid-point of each month. Instantaneous values were derived by linear interpolation.

Piako

Month	Flow (m3/s)	DIN mg	DRSi	POC mg	PON mg
	m3/s	N/m3	mg Si/m3	C/m3	N/m3
Jan	2.7174	1736	9333.333	5484	914
Feb	1.9069	1439	9333.333	4062	677
Mar	1.8459	1592	9333.333	4458	743
Apr	2.3677	3326	9333.333	4638	773
May	4.2516	2267	9333.333	5346	891
Jun	10.7587	2827	9333.333	6300	1050
Jul	16.5964	3474	9333.333	5772	962
Aug	14.4429	2969	9333.333	5928	988
Sep	10.4662	2287	9333.333	6156	1026
Oct	7.6217	2357	9333.333	5814	969
Nov	3.8338	1865	9333.333	5622	937
Dec	4.0471	1962	9333.333	6348	1058

Waitoa

Month	Flow (m3/s)	DIN mg	DRSi	POC mg	PON mg
	m3/s	N/m3	mg Si/m3	C/m3	N/m3
Jan	2.3657	1889	9333.333	3666	611
Feb	1.7952	1724	9333.333	3570	595
Mar	1.7935	1978	9333.333	3654	609
Apr	2.1166	2991	9333.333	4548	758
May	3.1856	3214	9333.333	3462	577
Jun	6.535	2744	9333.333	4116	686
Jul	10.057	3205	9333.333	4734	789
Aug	9.4788	3113	9333.333	4692	782
Sep	7.1553	3046	9333.333	4476	746
Oct	6.5921	2772	9333.333	4824	804
Nov	3.454	2415	9333.333	3786	631
Dec	3.6359	1864	9333.333	4998	833

Waihou

Month	Flow (m3/s)	DIN mg N/m3	DRSi mg Si/m3	POC mg C/m3	PON mg N/m3
Jan	33.7186	1022	9333.333	744	124
Feb	33.5109	917	9333.333	660	110
Mar	36.2237	981	9333.333	564	94
Apr	35.7486	986	9333.333	864	144
May	37.8356	1017	9333.333	582	97
Jun	46.6657	1164	9333.333	1560	260
Jul	52.486	1223	9333.333	1956	326
Aug	52.0114	1153	9333.333	1734	289
Sep	48.347	1160	9333.333	1398	233
Oct	43.4204	1167	9333.333	1374	229
Nov	37.7643	1047	9333.333	1002	167
Dec	37.9368	1065	9333.333	900	150

Ohinemuri

Month	Flow (m3/s)	DIN mg N/m3	DRSi mg Si/m3	POC mg C/m3	PON mg N/m3
Jan	6.4878	290	9333.333	816	136
Feb	7.1377	408	9333.333	1170	195
Mar	10.5711	503	9333.333	1158	193
Apr	10.5818	879	9333.333	720	120
May	10.9482	621	9333.333	690	115
Jun	18.4919	743	9333.333	1086	181
Jul	20.4569	710	9333.333	2622	437
Aug	18.1496	789	9333.333	762	127
Sep	16.5295	679	9333.333	702	117
Oct	12.4744	554	9333.333	786	131
Nov	7.8325	454	9333.333	846	141
Dec	9.5612	414	9333.333	714	119

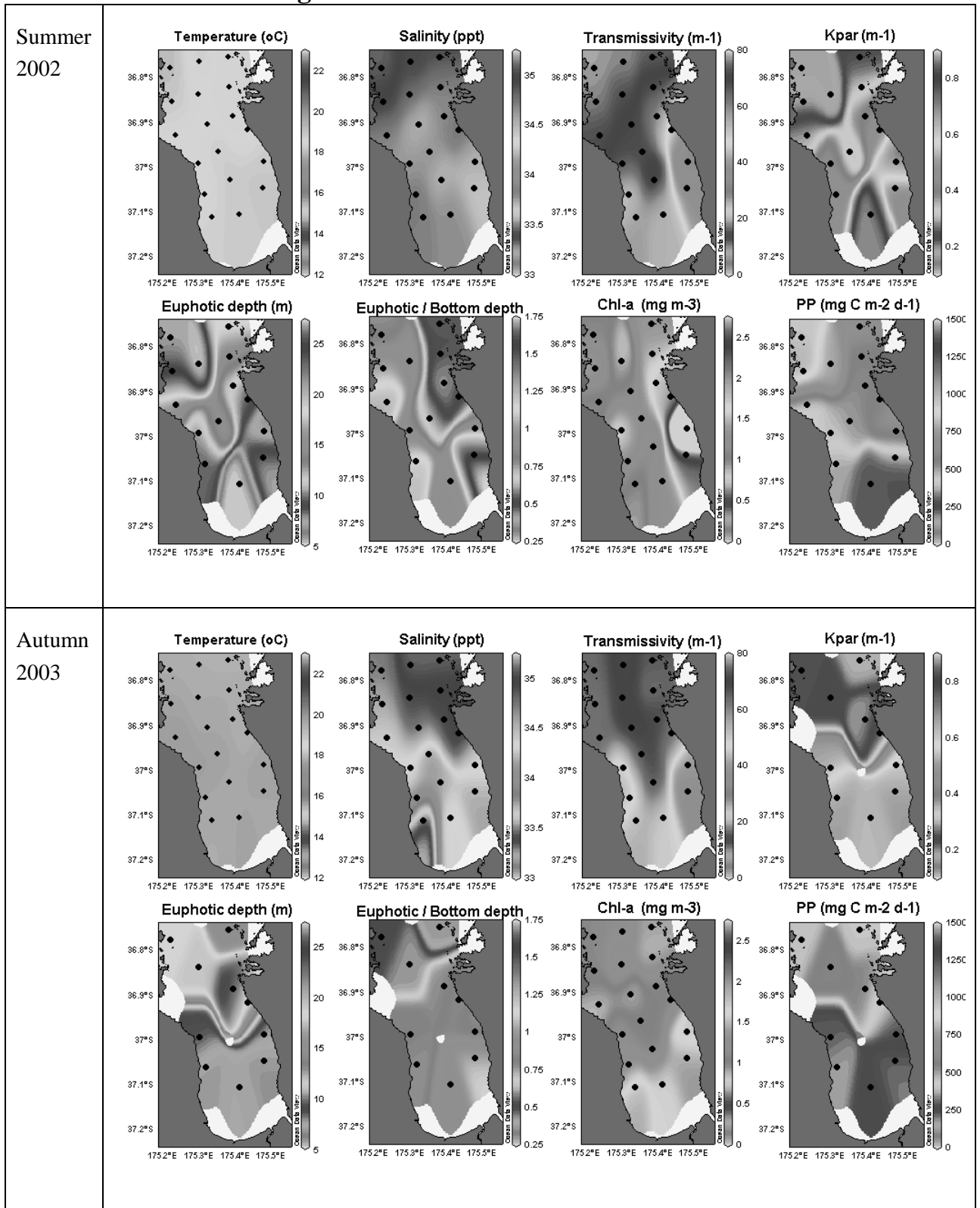
### Kaueranga

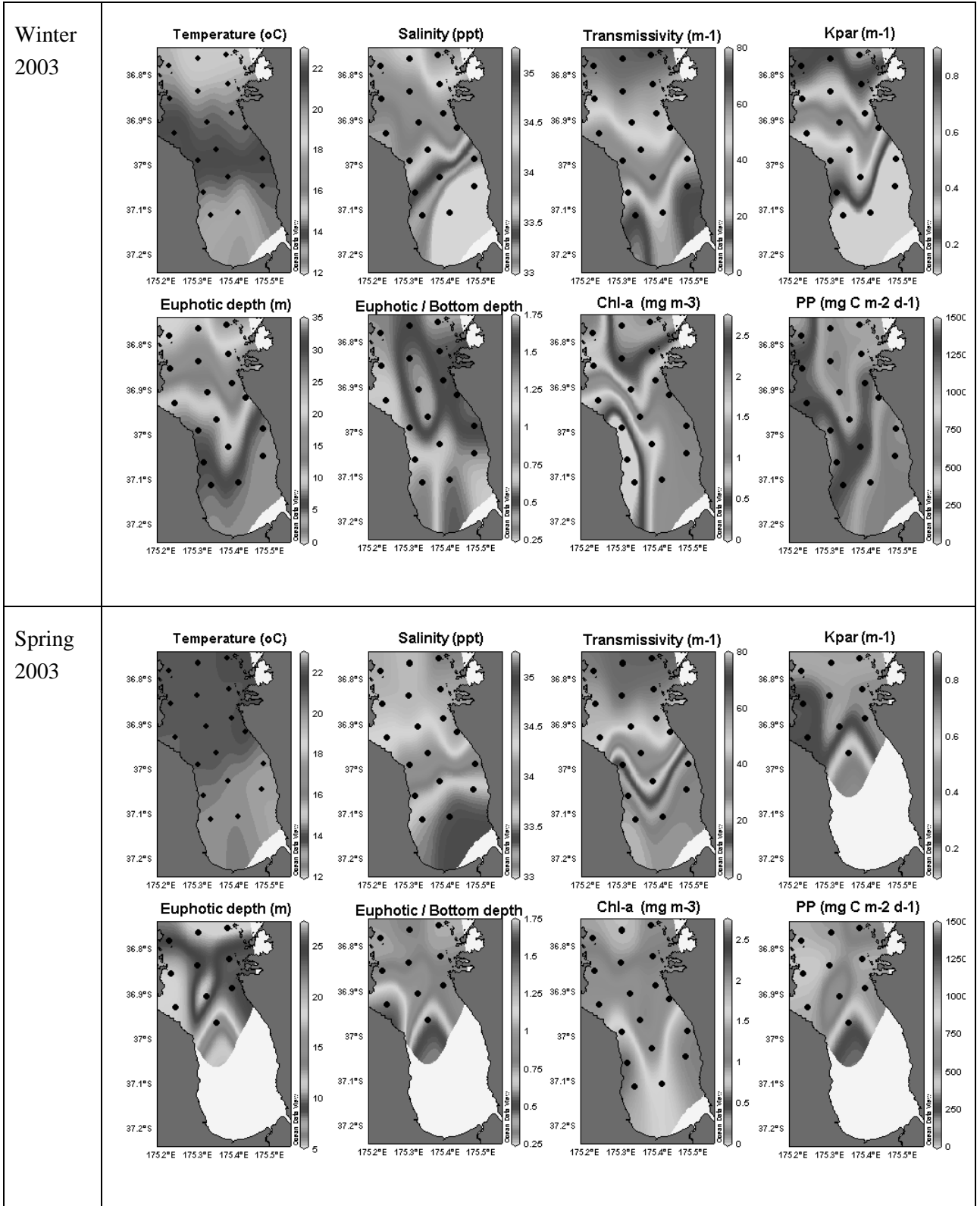
Month	Flow (m3/s)	DIN mg N/m3	DRSi mg Si/m3	POC mg C/m3	PON mg N/m3
	m3/s	N/m3	Si/m3	C/m3	N/m3
Jan	3.5696	60	9333.333	816	136
Feb	4.3726	17	9333.333	1074	179
Mar	6.0833	19	9333.333	1134	189
Apr	6.0736	81	9333.333	1530	255
May	5.6224	38	9333.333	270	45
Jun	9.0388	83	9333.333	774	129
Jul	10.6793	123	9333.333	540	90
Aug	9.4128	96	9333.333	594	99
Sep	8.1845	93	9333.333	936	156
Oct	5.4924	51	9333.333	552	92
Nov	4.4274	20	9333.333	306	51
Dec	4.0414	36	9333.333	444	74

### Thames Sewage discharge

Month	Flow (m3/s)	DIN mg N/m3	DRSi mg Si/m3	POC mg N/m3	PON mg N/m3
	m3/s	N/m3	Si/m3	N/m3	N/m3
Jan	0.05	17000	0	0	13000
Feb	0.05	17000	0	0	13000
Mar	0.05	17000	0	0	13000
Apr	0.05	17000	0	0	13000
May	0.05	17000	0	0	13000
Jun	0.05	17000	0	0	13000
Jul	0.05	17000	0	0	13000
Aug	0.05	17000	0	0	13000
Sep	0.05	17000	0	0	13000
Oct	0.05	17000	0	0	13000
Nov	0.05	17000	0	0	13000
Dec	0.05	17000	0	0	13000

**8. Appendix B. Summary illustrations of the results from the individual cruises from which light-attenuation was inferred.**





Summer  
2003

